Synthesis and Development of Compounds for Nonlinear Absorption of Light

Tomas Kindahl

Doctoral thesis

Department of Chemistry
Umeå University
Umeå, Sweden 2012

ISBN: 978-91-7459-503-1
Electronic version available at http://umu.diva-portal.org/
Printed by VMC-KBC, Umeå Universitet
Umeå, Sweden 2012

Author
Tomas Kindahl

Title
Synthesis and Development of Compounds for Nonlinear Absorption of Light

Abstract
High-intensity light — for instance that from a laser — can be destructive, not only to the human eye, but also to equipment such as imaging sensors and optical communication devices. Therefore, effective protection against such light is desirable. A protection device should ideally have high transmission to non-damaging light, and should also be fast-acting in order to effectively stop high-intensity light.

In working towards a protection device, there is a need to conduct fundamental research in order to understand the processes involved. One of the photophysical processes of special interest in the field of optical power limiting (OPL) is reverse saturable absorption, where a compound in an excited state absorbs light more strongly than it does in its ground state.

In this work, several novel organoplatinum compounds for OPL, rationally designed to have a strong reverse saturable absorption, have been synthesized. The compounds have been analyzed using linear and nonlinear absorption spectroscopy, luminescence spectroscopy, and quantum chemistry calculations to gain further knowledge regarding their photophysical properties.

In addition to this fundamental research, the absorption capabilities of some of these compounds indicate that they can be used for OPL applications. Consequently, compounds from these studies have been incorporated into a sol–gel glass that could be used in optical systems.

Keywords
Platinum acetylide, nonlinear absorption, optical power limiting, oxazole, quantum chemistry calculation, quantum chemical calculation, triplet absorption

Contents

List of papers

I Eirik Glimsdal, Marcus Carlsson, **Tomas Kindahl**, Mikael Lindgren, Cesar Lopes and Bertil Eliasson. Luminescence, Singlet Oxygen Production, and Optical Power Limiting of Some Diacetylide Platinum(II) Diphosphine Complexes. J. Phys. Chem. A, 114, 3431-3442, **2010**

II **Tomas Kindahl**, Pål Gunnar Ellingsen, Cesar Lopes, Carl Brännlund, Mikael Lindgren and Bertil Eliasson. Photophysical and DFT Characterization of Novel Pt(II)-coupled 2,5-Diaryloxazoles for Nonlinear Optical Absorption. Accepted with minor revisions in J. Phys. Chem. A. 2012-09-24.

III **Tomas Kindahl**, Cesar Lopes and Bertil Eliasson. Synthesis, optical power limiting, and calculations of triplet–triplet absorption by density functional theory of three novel Pt(II)diacetylide chromophores. Submitted to Tetrahedron Lett.

IV Denis Chateau, Frédéric Chaput, Cesar Lopes, Mikael Lindgren, Carl Brännlund, Johan Öhgren, Nikolay Djourelov, Patrick Nedelec, Cedric Desroches, Bertil Eliasson, **Tomas Kindahl**, Frédéric Lerouge, Chantal Andraud and Stephane Parola. Silica Hybrid Sol–Gel Materials with Unusually High Concentration of Pt–Organic Molecular Guests: Studies of Luminescence and Nonlinear Absorption of Light. ACS Appl. Mater. Interfaces, 4, 2369-2377, **2012**.

V **Tomas Kindahl**, Patrick Norman and Bertil Eliasson. A TD-DFT study of triplet state absorption of platinum(II) complexes with ethynyl-diaryloxazole ligands. Manuscript to be submitted to Comp. Theor. Chem.

Author's contributions

Paper I: Quantum chemical calculations, minor writing.
Paper II: Planning, synthesis, part of photophysical characterization, quantum chemical calculations, major writing.
Paper III: Planning, synthesis, quantum chemical calculations, major writing.
Paper IV: Synthesis of chromophores, minor writing.
Paper V: Planning, quantum chemical calculations, major writing.

Abbreviations

α-NPO	2-(1-naphthyl)-5-phenyloxazole
APTES	(3-aminopropyl)triethoxysilane
Boc	*tert*-butyloxycarbonyl
DABCO	1,4-diazabicyclo[2.2.2]octane
DFT	density functional theory
DMF	dimethylformamide
dppe	1,2-bis(diphenylphosphino)ethane
GLYMO	(3-glycidoxypropyl)trimethoxysilane
HOMO	highest occupied molecular orbital
IC	internal conversion
ISC	intersystem crossing
LUMO	lowest unoccupied molecular orbital
MO	molecular orbital
MTEOS	methyltriethoxysilane
NIS	N-iodosuccinimide
NMR	nuclear magnetic resonance
OPL	optical power limiting
OPO	optical parametric oscillator
PMMA	poly(methyl methacrylate)
PPO	2,5-diphenyloxazole
RMSE	root mean square error
RSA	reverse saturable absorption
S_n	n^{th} singlet state
τ_f	fluorescence lifetime
τ_{ph}	phosphorescence lifetime
T_n	n^{th} triplet state
TBAF	tetrabutylammonium fluoride
TBDPS	*tert*-butyldiphenylsilyl
TDDFT	time-dependent density functional theory
Tf	trifluoromethylsulfonyl
THF	tetrahydrofuran
TIPS	triisopropylsilyl
TLC	thin layer chromatography
TMS	trimethylsilyl
TPA	two-photon absorption
Ts	*p*-toluenesulfonyl
UV	ultraviolet

Introduction

Photophysics

The absorption and emission of light by matter can result in and be described by a number of processes. A convenient way to summarize those processes is by the use of a Jablonski diagram (Figure 1).

Electrons can be in one of two spin states denoted α and β. If all electrons in a system are paired with regard to their spin, the system is denoted a singlet state. If one electron is unpaired, as for example in radical species, the system is denoted a doublet state, and if there are two unpaired electrons, the system is denoted a triplet state.

Normal absorption is represented by *a* in the diagram. One photon is absorbed by the chromophore, and the system is electronically excited from its lowest singlet state (S_0) to a higher singlet state (S_n). If the excitation results in reaching state S_2 or higher, it is very common that rapid thermal relaxation to S_1 occurs (*b*). The phenomenon of fluorescence emanating only from the S_1 state, regardless of the initially reached state, is referred to as Kasha's rule;[1] however, many exceptions to this rule are known.[2]

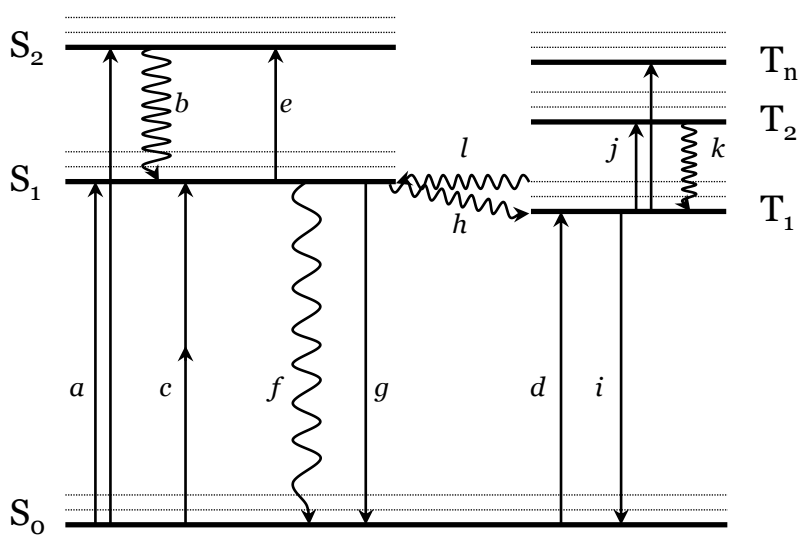

Figure 1. Jablonski diagram. See text for legend.

The simultaneous absorption of two photons, termed "two-photon absorption" (TPA), can occur at high light intensities (path *c*). The two photons may or may not be of the same energy, and are absorbed at the sum of their individual energies. TPA was predicted to be possible by Nobel laurate Maria Göppert-Mayer in 1931,[3] but first demonstrated some 30 years later.[4] There are many uses for TPA, for example two-photon microscopy,[5-6] microfabrication,[7-9] photodynamic therapy,[10-12] and optical power limiting.[13-15]

The spin-forbidden direct excitation from S_0 to T_1 (path *d*) has also been observed for platinum compounds, but is normally of very low intensity and can usually be disregarded.[16]

Once the S_1 state has been reached, a number of events can take place. Absorption can occur anew to give a higher singlet state (path *e*), with the same fate as discussed above. Relaxation to the ground state, either thermally, termed internal conversion (IC), or by fluorescence (path *f* and *g*, respectively) is possible. Yet another possibility is the intersystem crossing (ISC) to the T_1 state (path *h*).

The conversion rate from S_1 to T_1 is usually low, typically ranging from 10^6 to 10^8 s^{-1}, due to quantum mechanical selection rules where the angular momentum must be preserved.[17] This allows for competing relaxation via other pathways. However, the ISC rate can be increased in two ways: the introduction of a group with a non-bonding electron pair allows for a S(n,π*) to T(π,π*) or S(π,π*) to T(n,π*) conversion, where the angular spin can be preserved with a change of type of the excited electron orbital. Formulated in the 1960's, this is now known as the El-Sayed rule.[18] The other way to enhance the ISC is by the so called heavy atom effect. In heavy atoms there is a strong coupling between the spin angular momentum and the orbital angular momentum of the electrons. This facilitates the conservation of angular momentum and, hence, increases the intersystem crossing rate.

In T_1, the lowest triplet state, several events may occur. The spin forbidden relaxation back to S_0 (path *i*) is slow, with rates typically ranging from 10^{-4} – 10^2 s^{-1}, and this relatively long lifetime allows for other pathways to take place. Absorption of a photon can excite the system to one of several, in energy closely spaced, higher triplet states (T_2 ... T_n) (*j*). Relaxation from those states to T_1 occurs rapidly via internal conversion (*k*). Another possibility is the thermal repopulation of the S_1 state (*l*); this can be detected as delayed fluorescence.

Apart from these single-molecule events, the excited molecules might also undergo bimolecular events such as collisional quenching. In such an event, the excited state is transferred between molecules, or converted into another excited state.

A common fate of molecules in the T_1 state dissolved in air-equilibrated solvents is collisional quenching by triplet oxygen, where the chromophore is

efficiently relaxed from T_1 to S_0 simultaneously as dissolved oxygen, being in a triplet state, is converted to its singlet state. The singlet oxygen thus formed is highly reactive, and such collisional quenching necessitates deoxygenation of solvents for phosphorescence measurements.

In order to provide a measure of the importance of a certain pathway, the notion *quantum yield* (Φ) is used. It is the fraction of expected to total events for the process. For example, if one third of the molecules in an excited state gives rise to fluorescence, while the other two thirds do not due to IC or other quenching, the fluorescence quantum yield is 0.33 or 33%. The same terminology is used for phosphorescence and photochemical reactions.

Optical power limiting

Most materials exhibit linear absorption when irradiated with light, corresponding to *a* in Figure 2, according to the Lambert-Beer law. When the light intensity on a sample increases, so does the transmitted light. However, with very high light intensities, the Lambert-Beer law no longer holds due to effects other than single-photon absorption. Those most relevant in this thesis are reverse saturable absorption (RSA), where a long-lived excited state absorbs more strongly than the ground state, and two-photon absorption, where a high photon flux increases the probability of simultaneous absorption of photons. This gives a non-linearity in the absorption, corresponding to curve *b*.

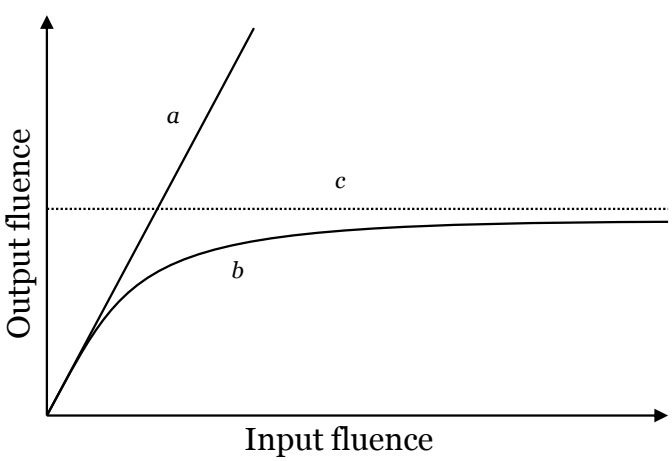

Figure 2. Schematic energy diagram showing the behaviour of an OPL material. *a)* Linearly absorbing material. *b)* OPL material. *c)* Clamping level.

The effect of power limiting is measured by passing a focused laser beam through a liquid or solid transparent matrix containing the OPL compound. By comparing the energy or fluence of the light entering the sample and the corresponding energy or fluence of the outgoing light, one acquires a measure of the power attenuation. For low intensities of light, typically below ca. 1 J/cm² for compounds studied in this project, the transmission should be high and linear as shown on the left side of curve *b*, Figure 2. At higher energies, non-linear effects are observed, and the curve flattens out (middle and right side of curve *b*).

If the transmitted fluence or energy for a sample never surpasses a certain value regardless of the light intensity, this is denoted the clamping level (*c*). As the clamping level is dependent on concentration, a low value is considered beneficial since the amount of material needed is smaller; otherwise, low solubility of the OPL chromophore might be restrictive to the power limiting as the concentrations needed for a good effect are relatively high.

While it is important that a compound shows a strong OPL effect, it is also important that the transparency is high at a low fluence of light in the wavelength range of interest. This is because a material incorporating such a compound should, in the ideal case, behave as a transparent filter and not distort or remove spectral information from transmitted light.

The power limiting capabilities are measured by using a powerful laser connected to a detector via a setup of lenses, filters and apertures (Figure 3).

The generated laser light may be subjected to a second harmonic generator (SHG) or optical parametric oscillator (OPO) in order to change the wavelength. A reference beam is collected through a semi-transparent mirror, as the pulse intensity can not be controlled precisely. The laser pulse is then subjected to a standardized set of lenses and apertures in order to obtain consistent results. After being focused in the sample of interest, the light pulse is converted into an electric signal in the detector and the intensity is measured.

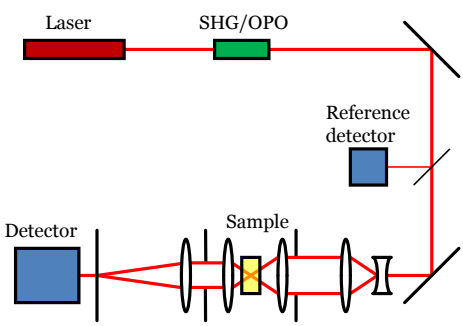

Figure 3. Schematic OPL measurement setup.

Structural motifs of OPL compounds

Compounds that have been used for OPL often share several features. Among these are large, conjugated π-systems like those of the compounds shown in Chart 1. Among investigated compounds that show OPL are C_{60},[19] metallophthalocyanines,[20-22] and Pt(II) alkynes.[23-25] Apart from the π-systems, many such compounds also contain metals for reasons explained below.

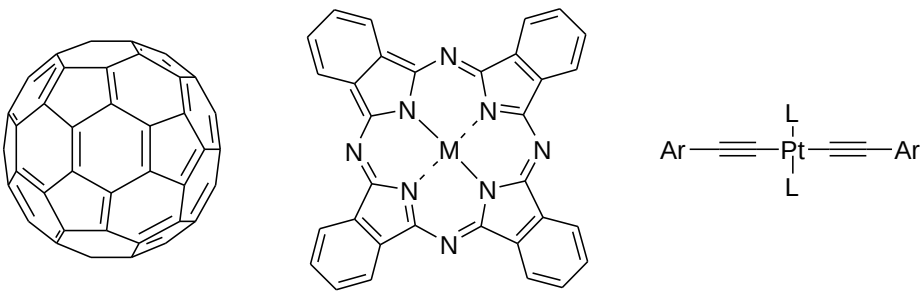

Chart 1. Examples of types of compounds that have been studied for OPL. C_{60}, a metallophthalocyanine, and a platinum acetylide.

All OPL compounds in this thesis share some common structural motifs. In a broad sense, the compounds are composed of three components: a chromophore containing an acetylene unit, a heavy metal ion, and ligands for the metal. Here, we have varied only the chromophore, while the metal and ligands used are platinum and tri-*n*-butylphosphine, respectively.

The role of platinum, as described in the photophysical background, is to provide a means of increasing the intersystem crossing rate. Other metals such as tin, lead, mercury, palladium and gold have been used for this purpose,[20, 26] but in this project we chose platinum for several reasons. One is that the platinum atom, for many compounds, only has a small effect on the absorption spectrum of the complex compared to the free ligand. This means that the spectrum of the ligand, if it is known, can be used to predict the spectrum of the complex. The OPL effect of platinum has in a few cases been shown to be better than for the corresponding compound with other heavy metals.[26] Finally, the C^{sp}-Pt(II) bond is stable and many such compounds has been stored for years in our laboratory without measurable degradation.

Ligands are needed to give the central platinum a stable electronic configuration. Many examples exist, such as arsines,[27] monophosphines,[27] bisphosphines,[28] bipyridines,[29] and terpyridines.[30] Depending on the ligands

chosen, the chemical and physical properties of the platinum complex can be modulated. Alkyl phosphines are more electron donating than diimine type ligands, and may be expected to influence electronic excitations and charge transfers. The solubility of the complexes can also be altered with the choice of ligand; space-filling alkyls often give better solubility in organic solvents than aryls. The square planar platinum complexes may be locked in a *cis* conformation with the use of bipyridines or bisphosphines such as dppe to prevent them from isomerizing to the *trans* isomer should they be unstable, while the *trans* isomer is usually stable and can be synthesized from *trans*-PtL_2X_2, where X is a halogen.

The conformation of the ligands, with regard to being either *cis* or *trans* in the square planar complex, has a large impact on the imaginary part of the third-order hyperpolarizability (γ) and therefore also on the two-photon absorption, which is dependent on γ.[31-32] In one isomeric pair, the *trans* compound showed an almost four-fold increase in the imaginary part of the third-order hyperpolarizability over the *cis* compound.[32] The conformation of synthesized compounds can be ascertained with the use of ^{31}P NMR, where the splitting of phosphorus peak by ^{195}Pt is greater in *cis* than in *trans* compounds.[33]

Two chromophores, bearing alkynyl scaffolds, are connected to the complexes studied in this work. The alkyne functionality provides a simple way of connecting the chromophore to the metal ion, as the synthesis is very mild. The C^{sp}-Pt(II) bond is air stable, and stable under mildly basic or acidic conditions.

The chromophores are the most important feature of the complex, as they dictate the various light absorption processes. The absorption of low intensity light in the intended wavelength range should be low to provide optical transparency. This, in general, imposes a limit on the size of the conjugated system. The triplet–triplet absorption should be strong and, again, in the intended wavelength range. A high two-photon cross section of the molecule is desirable, although not necessary.

The position of the alkyne on the chromophore is important. There should ideally be a strong electronic coupling between the π-system of the chromophore and the metal ion to promote the ISC. For example, an aryls connected to the 4-position of an oxazole is not conjugated with the rest of the system, and the absorption spectrum of such compounds are overlays of the separate moieties.[34] Such a position would likely be a bad choice for coupling to platinum via an alkyne.

The alkyne-bearing chromophore should preferably be easily synthesized, and should be photostable and chemically stable to withstand the harsh conditions of strong laser light.

Quantum chemistry calculations

Computational methods have provided a complement to the more traditional experimental chemistry, and can provide insight into many molecular and electronic processes, such as reaction and conformational energy barrier height, bond strength, and electronic transitions.

Many different computational methods exist, *e.g*. Molecular Mechanics, ab-initio methods such as Hartree-Fock, semi-empirical methods such as AM1 and PM3, Density Functional Theory (DFT), and Configuration Interaction; each having their distinct advantages and disadvantages. DFT is an attractive choice, since it is computationally cheap compared to other methods that include electron correlation, and produces accurate results for many systems. DFT is especially advantageous for transition metals compared to HF and post-HF methods.[35]

While ab-initio methods deal with the wave functions of a system, DFT deals with the electron density. Calculating the electron density of a system is a simpler task than calculating the total wavefunction. In addition, the electron density, as opposed to the wavefunction, has a physical meaning and can intuitively be understood. The function relating electron density to energy is unfortunately not known, but an abundance of approximations that can be used have been developed.[36-43]

In essence, the energy of a system is determined by:

$$E = E^T + E^V + E^J + E^{XC} \quad (1)$$

where E^T is the kinetic energy of the electrons, E^V is a potential energy term that includes electron-nucleus attraction and nucleus-nucleus repulsion, E^J is the electron-electron Coulomb repulsion, and E^{XC} is the exchange-correlation.[44] The Born-Oppenheimer approximation is typically applied, so the nuclear kinetic energy is not considered. The terms E^T, E^V and E^J can be evaluated in a classical sense, and this subject is discussed comprehensively in textbooks.[35] The most interesting term is the exchange-correlation, which encompasses quantum mechanical and classical electron interactions that are not captured in the other terms. The E^{XC} term can also be fitted with empirical parameters to better model experimental results. There is one major drawback with electron-correlation: the exact functional is not known, and must be approximated. Even worse, there is no known systematic approach to improve the approximation of E^{XC}. Oftentimes, the exchange-correlation is evaluated against sets of experimental data, but even with good correlation there is no guarantee that the term is valid in a strict sense, because the fit could come from fortuitous cancellation of errors.[45]

DFT can be used to calculate and predict electronic transitions to excited states by a method called Time-Dependent Density Functional Theory

(TDDFT). In a very simplified qualitative sense, the frequency dependent mean polarizability can be solved with regard to frequency and oscillator strength.[45] The obtained excitation energies can then, for example, be used to predict absorption spectra. TDDFT is routinely used today and usually gives good experimental agreement with lower excitations.

Results and discussion

Paper I

It was hypothesized in our group that platinum complexes bearing thiophene rings and methoxy substituted phenyl rings would increase T_1–T_n absorption compared to unsubstituted phenyls. In addition to this, we wanted to gain knowledge about the energy dissipation and radiative emission from such complexes.

The synthetic strategy outlined here was developed earlier, and was also used in Paper III and Paper IV. Therefore, it will be explained somewhat more in detail here although my main contribution to the paper was the quantum chemical calculations discussed at the end of this chapter.

Four novel platinum complexes were prepared in our laboratory. Three of the compounds carry thiophene rings at different positions in their ligands, and one incorporates methoxy groups in addition to a thiophene ring (Chart 2).

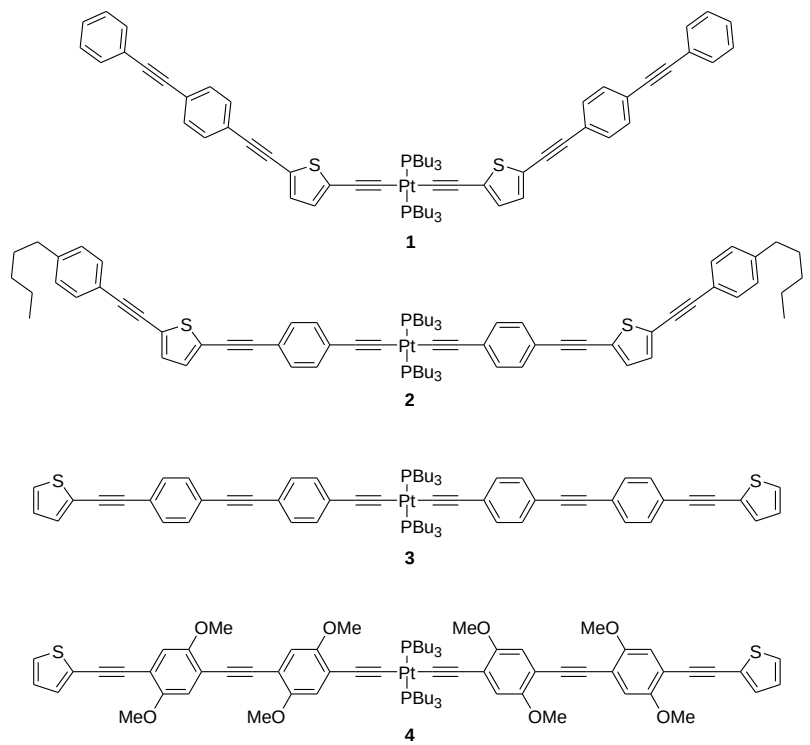

Chart 2. Novel thiophene-containing platinum complexes **1**-**4**.

The versatile building blocks **7** and **8** were prepared according to Scheme 1. The reaction is robust, although yields are low due to the fact that the coupling is not monoselective.

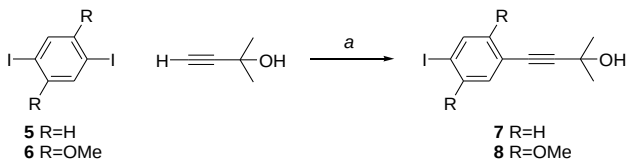

Scheme 1. Synthesis of building blocks **7** and **8**. *a*) $Pd(PPh_3)_2Cl_2$, CuI, PPh_3, DMF/Et_3N (45% and 47% respectively).

Pt complexes **3** and **4** were prepared by iterative Sonogashira coupling-deprotection of compounds **7** and **8**, respectively, with 2-ethynylthiophene (**9**), Scheme 2.

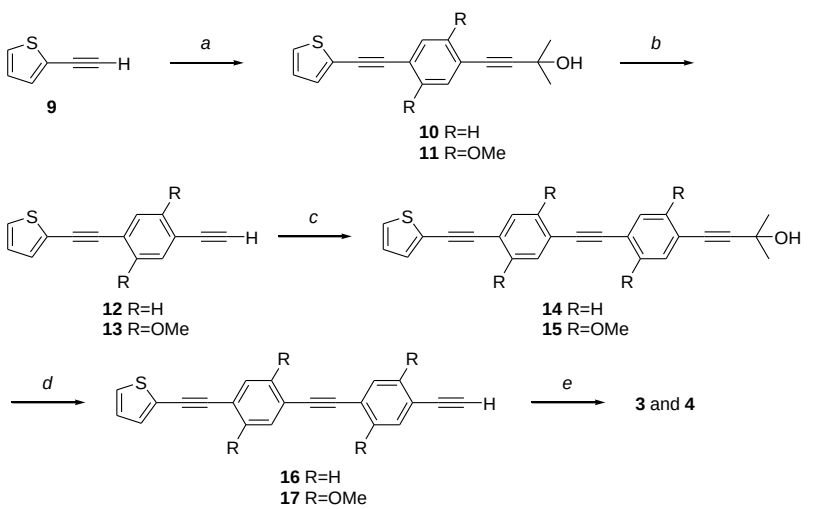

Scheme 2. Synthesis of **3** and **4**. *a*) **7** or **8**, $Pd(PPh_3)_2Cl_2$, CuI, PPh_3, THF/Et_3N (89% for both compounds); *b*) KOH, toluene (89%; 84%); *c*) Conditions as *a* (88%; 64%); *d*) Conditions as *b* (98%; 87%); *e*) *trans*-$Pt(PBu_3)_2Cl_2$, CuI, Et_3N/THF (quant.; 60%).

Compound **2** was synthesized according to Scheme 3, starting with the Sonogashira coupling of 2,5-diiodothiophene (**18**) to alcohol **19**. Coupling of the remaining iodine with 4-pentylphenylacetylene as the partner gave **21**, and, after deprotection, **22**. Again, a coupling-deprotection sequence gave compound **23** and then **24**. The alkyne ligands were connected to *trans*-

$Pt(PBu_3)_2Cl_2$ under Sonogashira-Hagihara conditions to give the desired Pt complex **2**.

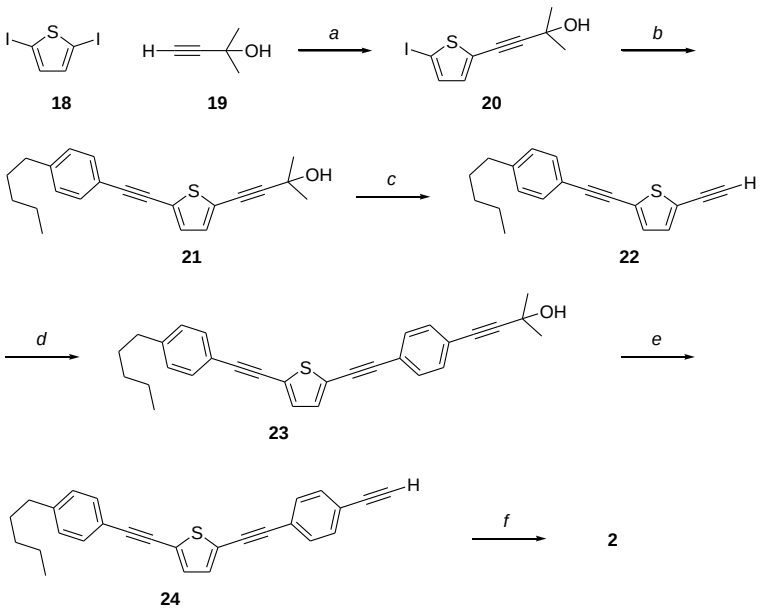

Scheme 3. Synthesis of compound **2**. *a*) $Pd(PPh_3)_2Cl_2$, CuI, PPh_3, THF/Et_3N (68%); *b*) Conditions as *a* (86%); *c*) NaH, toluene (29%); *d*) Conditions as *a* (70%); *e*) KOH, toluene (66%); *f*) *trans*-$Pt(PBu_3)_2Cl_2$, CuI, Et_3N/THF (72%).

In a similar fashion, compound **1** was synthesized using the same unsymmetric thiophene **20** that was used in the synthesis of compound **2**, summarized in Scheme 4.

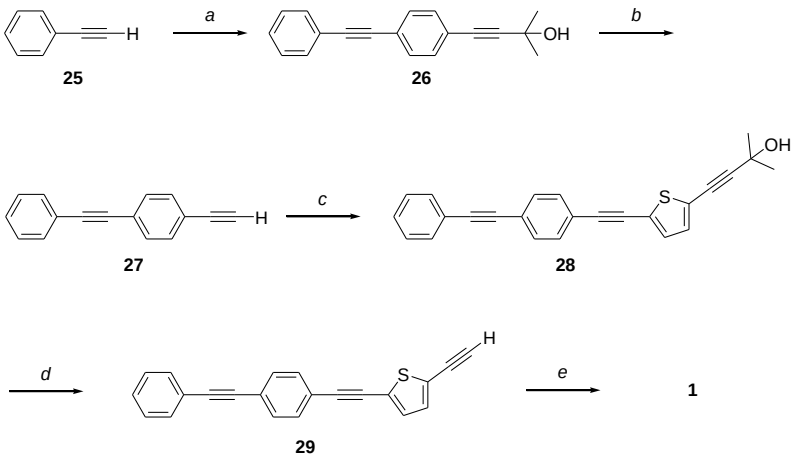

Scheme 4. Synthesis of compound **1**. *a*) **7**, $Pd(PPh_3)_2Cl_2$, CuI, PPh_3, THF/Et_3N; *b*) KOH, toluene (63% over two steps); *c*) **20,** $Pd(PPh_3)_2Cl_2$, CuI, PPh_3, THF/Et_3N (60%), *d*) Conditions as *b* (78%); *e*) *trans*-$Pt(PBu_3)_2Cl_2$, CuI, Et_3N/THF (86%).

After synthesis, the required compounds were characterized with photophysical methods. All were found to have an absorption band containing two overlapping peaks (Figure 4a). The closer the thiophene ring is to the Pt atom, the smaller the S_0-S_1 gap. However, the gap for **4** is even smaller than for **1** even though the thiophene rings in the latter compound are situated at distal positions, showing that the substitution pattern can have a profound effect on the absorption spectrum of this type of compound.

The same trend is seen for the fluorescent emission of the compounds (Figure 4b, 400-500 nm). As is commonly observed for platinum(II) acetylides, the fluorescence quantum yield is low, at or below 5%.

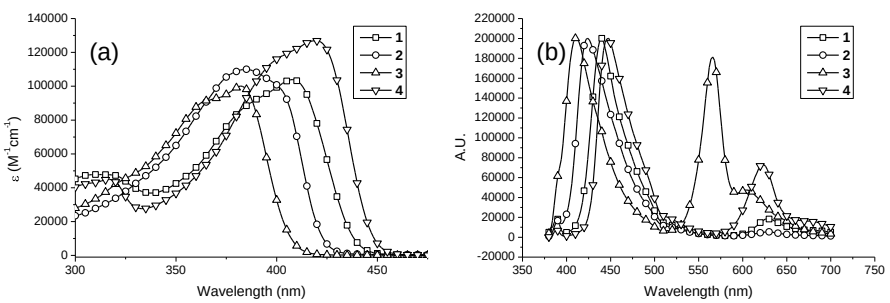

Figure 4. (a) Absorption and (b) emission of compounds **1**-**4**.

The phosphorescence differs between the compounds; compound **1**, **2** and **4** emits with a maximum >600 nm, while **3** has its maximum at 566 nm. The band shape of **3,** with a weaker peak near 600 nm, suggests a different state than those of the other compounds, or two emitting vibronic states.

The phosphorescence efficiency differs substantially between the compounds, where compound **3** emits more than the other compounds, especially compared to compound **2**. The spectra in Figure 4b are normalized to fluorescence, but as the fluorescence quantum yield and band shape are similar, the phosphorescence spectral area can be used for a qualitative discussion. There are at least two plausible explanations for why compound **2** is such a weak phosphophore: the ISC rate from S_1 to T_1 (or T_n) could be small, or there could exist an efficient non-radiative relaxation pathway from T_1 to S_0. It can be inferred from the phosphorescence lifetimes of compounds **2** and **3** (Table 1), where weaker-emitting **2** has the longer lifetime of the two, that it is likely not a radiationless T_1–S_0 ISC that attenuates the phosphorescence of **2**.

Table 1. Phosphorescence lifetimes of compounds **1**-**4**.

Compound	τ_{ph} (μs)
1	27
2	280
3	140
4	300

It is well known that triplet states of Pt complexes in solution can be efficiently quenched by dissolved oxygen, in a process where the oxygen, in its natural triplet state, is excited to a singlet state.[46] The generated singlet oxygen can then phosphoresce in its relaxation to the triplet state, and this phosphorescence can be detected at 1270 nm. This procedure, using oxygen-equilibrated solvents, was performed on **1**-**3**, and it was found that the oxygen phosphorescence intensity followed that of the corresponding compound. This again suggests that the T_1 state of **2** is not emptied by radiationless relaxation, but rather that the probability to reach T_1 from S_1 differs between the compounds.

The OPL capabilities of compounds **1**-**4** were measured at 532 and 600 nm, and all compounds showed strong limiting with a clamping levels at approximately 4 and 5 μJ at the respective wavelength. However, there was no significant improvement over an all-benzenoid version of the compounds (denoted PE3 in Paper I).

We investigated the influence of the geometry of compounds **1** and **2** on various properties using DFT calculations. Simplified structures of the compounds were used, where tributylphosphine was exchanged for trimethylphosphine, and the pentyl group of **2** was exchanged for a

hydrogen. The functional and basis set were chosen as a tradeoff between speed and accuracy.[47-48] The main findings are summarized in Table 2.

For **1**, five different conformations were used as starting points in the geometry optimization, varying in the angle between the ligand and the Pt-P bond, and in the relationship of the thiophene rings. It must be emphasized that *cis* and *trans* here refer to the orientation of the sulfur atoms of the rings, and not to the configuration of Pt. The conformations are denoted pl-pl-trans ("planar-planar-trans"), pl-pl-cis, perp-perp-trans ("perpendicular-perpendicular-trans"), perp-perp-cis, and pl-perp. All were optimized to local minima, although spaced closely in energy, with a difference of only 0.63 kJ/mol between pl-pl-trans as the most stable conformer, and perp-perp-cis as the least stable conformer. The barrier heights between the conformers were not quantitated, but they are not insignificant as local minima were indeed found. The conformations are shown in Figure 5.

Table 2. Calculated vertical excitation energies for compounds **1** and **2**.

Compound[a]	Conformation	Relative energy (kJ/mol)	Wavelength (nm)[b]	Oscillator strength
1	pl-pl-trans	0	466	3.64
	pl-pl-cis	0.08	463	3.15
	pl-perp	0.42	430	4.10
	perp-perp-trans	0.59	429	3.99
	perp-perp-cis	0.63	425	3.43
2	perp-perp-trans	0	425	4.34
	pl-perp	1.88	430	4.33
	pl-pl-trans	3.56	454	3.95

[a] Structure simplified according to text. [b] Strongest transition.

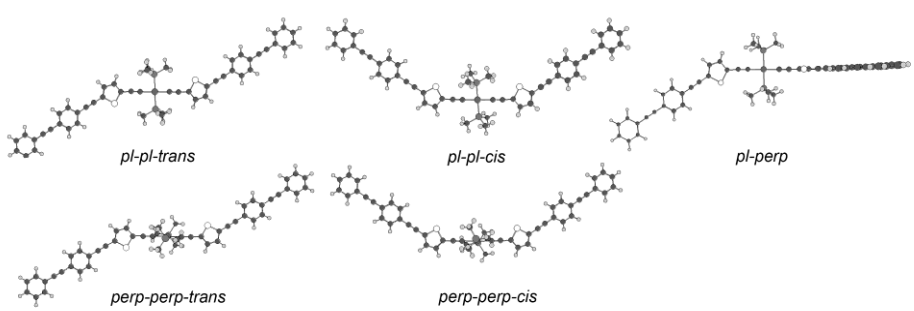

Figure 5. Conformers of **1**.

The five different geometries were further characterized with regard to their electronic transitions, using TDDFT. It was found that the S_0–S_1 transition did not differ much in energy between the *cis* and the *trans* conformations; the *trans* transitions were a few nm longer in wavelength than the corresponding *cis* transitions, and had a slightly larger oscillator strength. A difference in excitation energy was however found for the planar and perpendicular conformations, with the former near 465 nm, and the latter near 427 nm, differing slightly with regard to *cis* and *trans* as described above. This is in accord with the experimental spectrum, where peaks at 408 nm and approximately 380 nm can be seen, given that the TDDFT excitation energy may not correspond to λ_{max} and that the calculated structures are simplified.

In hindsight, another explanation would be that the experimental peaks have their origin in different vibrational states of the compound. The peaks are separated by approximately 1800±300 cm^{-1}, consistent with aromatic vibrations.[49]

Interestingly, there is only one major transition of the "pl-perp" conformation, whereas two similar—although not identical—transitions would be expected if the ligands were not interacting. This is not immediately obvious since the π-systems of the ligands are perpendicular to each other. Therefore, an interaction between the ligands seems to be mediated by the platinum atom.

Corresponding calculations were performed for **2**, but the *cis* conformers were not taken into account as they were expected to be very similar to the *trans* conformers. In this case, the opposite relation to compound **1** was found with regard to energy minima. Here, the all-perpendicular structure (perp-perp-trans) was found to be 3.56 kJ/mol below the all-planar (pl-pl-trans) structure, with the pl-perp conformer being almost exactly the average in energy of those two former conformers. The presence of thiophene rings in proximity to the platinum atom seems to stabilize the all-planar structure; however, it must be noted that the energy difference may be quite different in the actual compounds due to structure simplifications and other factors.

With regard to excitation energy, the same trend as for **1** was found for **2**, where the all-planar conformation has a smaller S_0–S_1 energy gap than the all-perpendicular conformation.

The excitations of **1** and **2** with the greatest oscillator strength were found to be dominated by HOMO–LUMO transitions. By visualizing the molecular orbitals of the all-perpendicular and the all-planar conformations, we found that the HOMO of them were almost identical (Figure 6). The LUMO, shown in Figure 7, is however vastly different, with a much greater coefficient on the central platinum atom for the all-planar conformation than for the all-perpendicular one. This could then imply that the ISC is more efficient from a planar conformation because of a greater spin-orbit coupling.

Unfortunately, this hypothesis appears not to have been experimentally tested, but could be an interesting subject for future research.

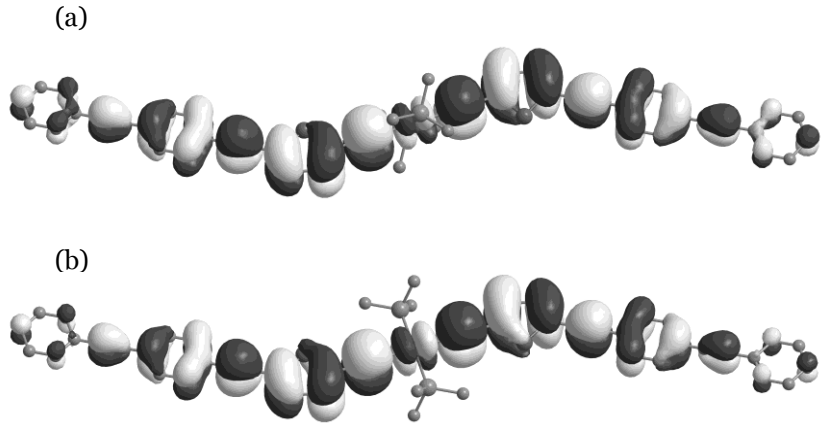

Figure 6. HOMO of compound **1** in the (a) perp-perp-trans and (b) pl-pl-trans conformations.

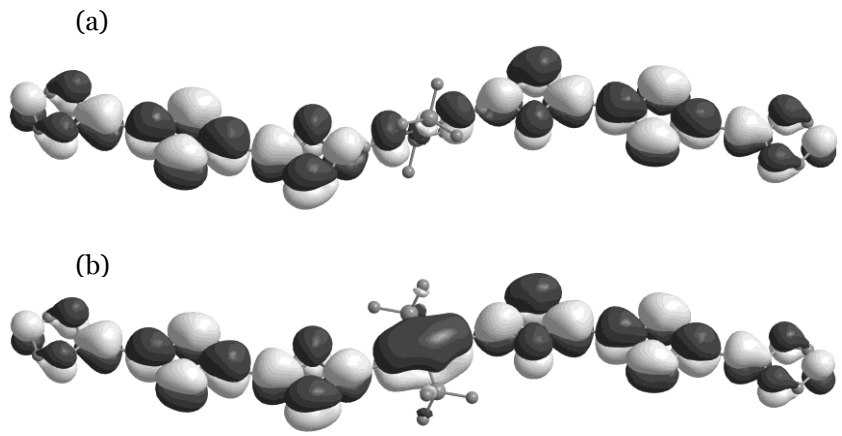

Figure 7. LUMO of compound **1** in the (a) perp-perp-trans and (b) pl-pl-trans conformations.

Paper II

The basis of this study comprised a rational approach to make compounds with a strong triplet absorption at wavelengths at and longer than 600 nm. The literature was examined for compounds with absorption near 550 nm,[50] keeping in mind that a red-shift is common upon coupling with platinum.[51] Among several interesting compounds, PPO with ε_t = 28 400 at 500 nm, and α-NPO with ε_t = 100 000 at 550 nm (Chart 3), were selected for further studies.

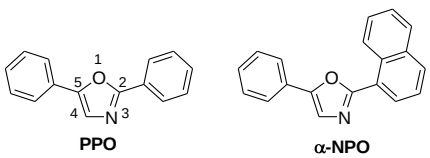

Chart 3. Chemical structures of compounds PPO and α-NPO.

The oxazoles in the work were synthesized by the Robinson-Gabriel cyclodehydration of β-ketoamides,[52-53] using phosphorus oxychloride in DMF. The β-ketoamide is made by the coupling of a 2-aminoacetophenone with an aroyl halide.

In the early stages of the project, we investigated the possibility to vary the substituents on the phenyl that ends up in the 5-position on the oxazole (Scheme 5), using acetophenone (**30**) as a model compound, with a plan to use other starting materials in the future. α-Keto halogenation with elemental bromine under acidic conditions gave 2-bromoacetophenone (**31**). The bromine was exchanged for an azide using sodium azide, and the corresponding azido compound **32** was Staudinger reduced[54] in the presence of *p*-toluenesulfonic acid trihydrate to give ammonium tosylate **33**. Preliminary work shows that the same procedure is possible using 4'-aminoacetophenone in a Sandmeyer type reaction to give 4'-iodoacetophenone as the starting material; however, commercial 4'-bromo-2-aminoacetophenone hydrochloride was used in the subsequent synthesis, and only the 2-aryl group of the oxazole was varied.

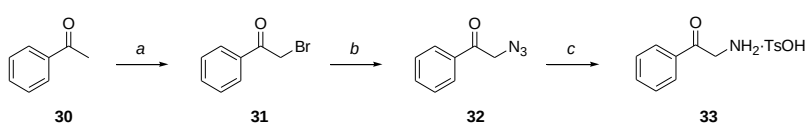

Scheme 5. Investigative synthesis of starting material **33**. *a*) Br_2, HBr, H_2O/MeOH (55%); *b*) NaN_3, KI, DMF (89%); *c*) $TsOH{\cdot}H_2O$, PPh_3, THF (69%).

Owing to the instability of 4'-bromo-2-aminoacetophenone in basic solution because of self-condensation,[55] the amino group was Boc protected before coupling to TMS-acetylene under Sonogashira conditions, as shown in Scheme 6. The amine was deprotected and salted out by generating HCl in situ from ethanol and acetyl chloride.[56]

All amide couplings were straight forward and were made either in CH_2Cl_2 using triethylamine as a base, or, later, under Schotten-Baumann conditions[57-58] (CH_2Cl_2 and aqueous bicarbonate).

Robinson-Gabriel cyclodehydration of the amides using phosphorus oxychloride in DMF afforded the oxazoles with a pendant TMS-protected alkyne in reasonable yields. The alkyne was deprotected using standard conditions of potassium carbonate in methanol.

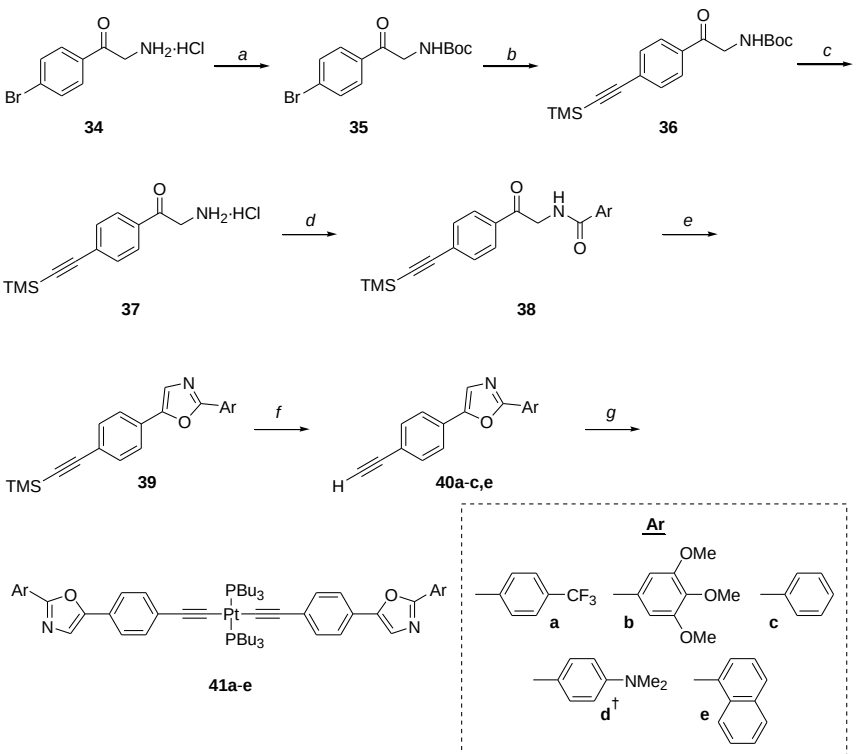

Scheme 6. Synthesis of platinum coupled 2,5-diaryloxazoles **41a-e**. *a*) Boc_2O, Et_3N, THF (quant.); *b*) TMS-acetylene, $Pd(PPh_3)_2Cl_2$, CuI, Et_3N, DMF (84%); *c*) AcCl, EtOH (83%); *d*) ArCOCl, Et_3N, CH_2Cl_2 (62%-quant.); *e*) $POCl_3$, DMF (83-93%); *f*) K_2CO_3, MeOH (68-79%); *g*) *trans*-$Pt(PBu_3)_2Cl_2$, CuI, Et_3N, THF (19-83%). †See Scheme 7.

In the case of the dimethylamino substituted aryl group, shown in Scheme 7, 4-nitrobenzoyl chloride was used as the partner in the amide coupling to give compound **42**. After cyclodehydration, the nitro group was reduced using zinc in acetic acid to give the corresponding aniline **44**. Tin(IV) chloride was also used and gave similar yields. Attempts to methylate the aniline under Eschweiler-Clarke conditions[59-60] gave a mixture of decomposition products; reductive amination using sodium cyanoborohydride and aqueous formaldehyde[61] functioned satisfactorily but was inconsistent in terms of having to feed the reaction with reagents. The best of the tested methods was exhaustive methylation with methyl iodide, then demethylation *in situ* by reacting with DABCO to give compound **45**.[62] Although the atom economy is very poor, the reaction proceeded efficiently and gave the desired terminal alkyne **40d** after deprotection.

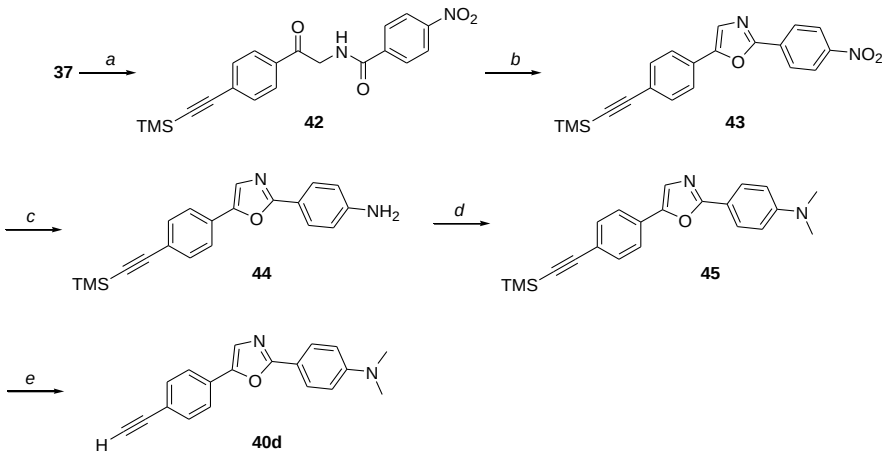

Scheme 7. Synthesis of compound **40d**. *a*) 4-nitrobenzoyl chloride, Et_3N, CH_2Cl_2 (62%); *b*) $POCl_3$, DMF (47%); *c*) Zn, AcOH (86%); *d*) MeI, DMF (85%); *e*) K_2CO_3, MeOH (79%).

The terminal alkynes were coupled to *trans*-$Pt(PBu_3)_2Cl_2$ using Sonogashira-Hagihara conditions[63-64] (copper(I) iodide and an amine base) in THF to give a small selection of Pt-coupled 2,5-diaryloxazoles: **41a-e**.

The Pt coupled oxazoles are stable when stored neat under bench-top conditions, but it was noticed that samples that were allowed to stand in solution, for example in NMR tubes or in vials after OPL measurements became degraded. To investigate what was formed, and how, a sample of **41c** was dissolved in THF and allowed to stand under air atmosphere and in light for several weeks. TLC and NMR indicated quantitative and clean conversion to two new compounds. The sample was chromatographed to give N-

formylbenzamide (**46**) and a compound tentatively identified as *trans*-[bis-(4-ethynylbenzoic acid) bis-tributylphosphine] platinum (**47**).

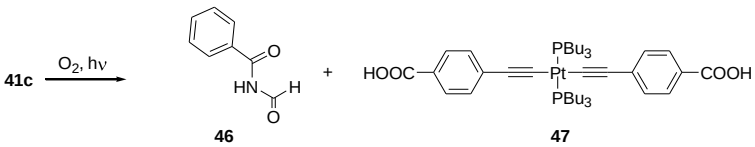

Scheme 8. Degradation of compound **41c** in air and light.

These compounds are in agreement with the product formed by singlet oxygen oxidation of the oxazole moiety.[65-67] As reported in Paper I, similar Pt-coupled chromophores generate singlet oxygen *via* quenching of the triplet state,[68] corroborating this conclusion. The UV spectrum of the degraded mixture of compounds is characteristically different from the one belonging to the pure compound, with peaks near 300 nm ($\varepsilon \approx 22000\ M^{-1}\ cm^{-1}$) and 345 nm ($\varepsilon \approx 40000\ M^{-1}\ cm^{-1}$) (Figure 8).

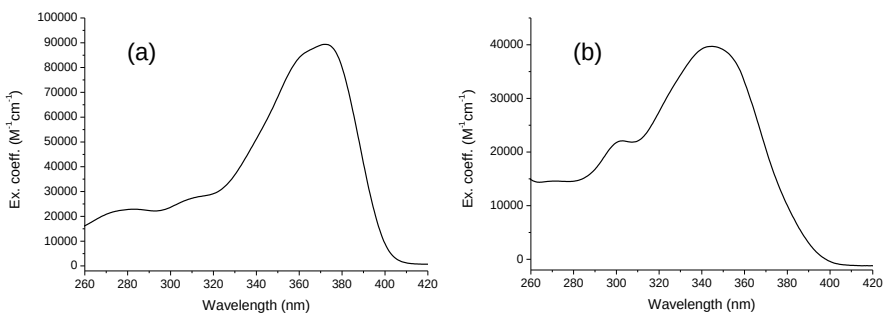

Figure 8. UV-vis spectra of (a) **41c**; (b) degraded products of **41c**

The synthesized alkynes were investigated using spectroscopic methods. The absorption spectra of **40a-e**, shown in Figure 9a, feature a broad peak from 300 nm to 350-400 nm depending on the substituent on the ring distal to the alkyne. The broad main absorption bands contain subfeatures; however, the general broadness suggests that the peaks originate in a wide selection of conformations.

Looking at the fluorescence spectra, we noticed that compound **40e** and especially **40c** gave sharper vibronic features than the three other compounds. Although it is not clear why this is the case for only those two, it does indicate that the conformational distribution in the S_1 state is smaller than that in the S_0 state, where the peaks are broader.[69]

The fluorescence quantum yields and fluorescence lifetimes are on the same order of magnitude as observed for the model compounds α-NPO and PPO (Table 3). The high quantum yields show that the internal conversion is relatively slow, and would allow for efficient intersystem crossing when coupled to a heavy atom.

Table 3. Fluorescence quantum yields and lifetimes of oxazole ligands **40a-e**, α-NPO and PPO.

Compound	Φ_f	τ_f
40a	0.61	1.31
40b	0.68	1.27
40c	0.59	1.08
40d	0.77	1.53
40e	0.75	1.62
α-NPO[a]	0.78	2.3
PPO[a]	0.7	1.6

[a] From ref. [70]

Upon coupling to platinum to form the corresponding *trans*-bisalkyne bisphosphine platinum complexes **41a-e**, the absorption spectra of all compounds are red-shifted to varying degrees (Figure 9b). This indicates that the conjugation of the alkyne ligand is extended onto and beyond the platinum atom. The amount of red-shift is not consistent over the compounds; for example, **40a** compared to **41a** shows a larger excitation energy difference than that of **40e** *vs.* **41e**. This suggested that the ligand-Pt interaction strength was modulated by the substitution pattern of the distal aryl.

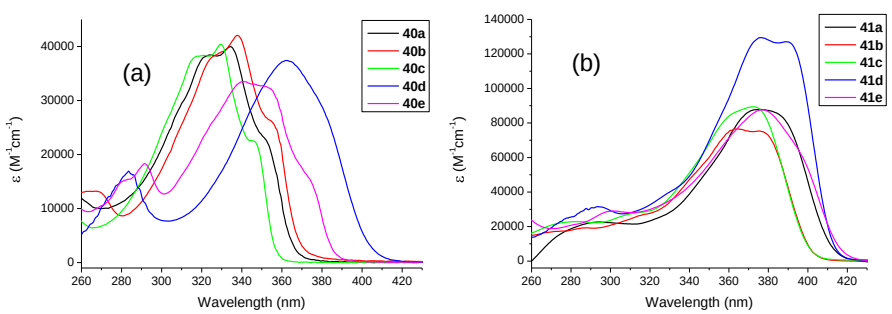

Figure 9. UV-vis absorption of (a) ligands **40a-e** and (b) Pt complexes **41a-e**.

The same reasoning can be applied when comparing the fluorescence spectra of the ligands and the Pt complexes, shown in Figure 10. The largest red-shift is seen in the trifluoromethyl pair **40a**/**41a**, and, surprisingly, a small

blueshift is seen in the dimethylamine pair **40e**/**41e**. With these two facts in mind, the Pt-ligand interaction strength was subsequently investigated *in silico* (*vide infra*). Measurements of fluorescence lifetimes together with detected phosphorescence indicate that the S_1 state of the Pt complexes is quickly depleted by ISC to T_1, and hence the quantum yields are low with a maximum of 1.7% for compound **41e**.

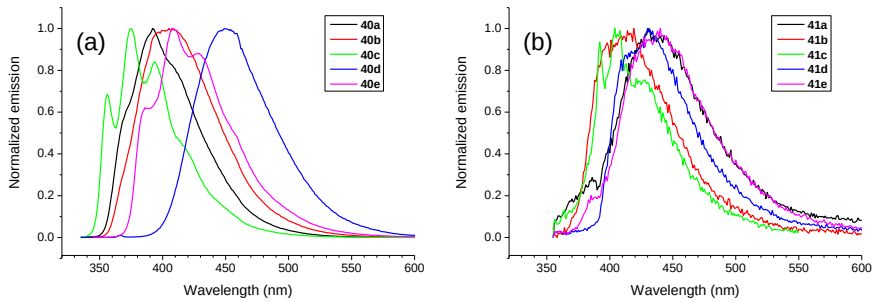

Figure 10. Normalized fluorescence from (a) ligands **40a-e** and (b) Pt complexes **41a-e**.

Phosphorescence of the Pt compounds was not detected in atmosphere-equilibrated solvents, but was observed after thorough degassing (Figure 11).

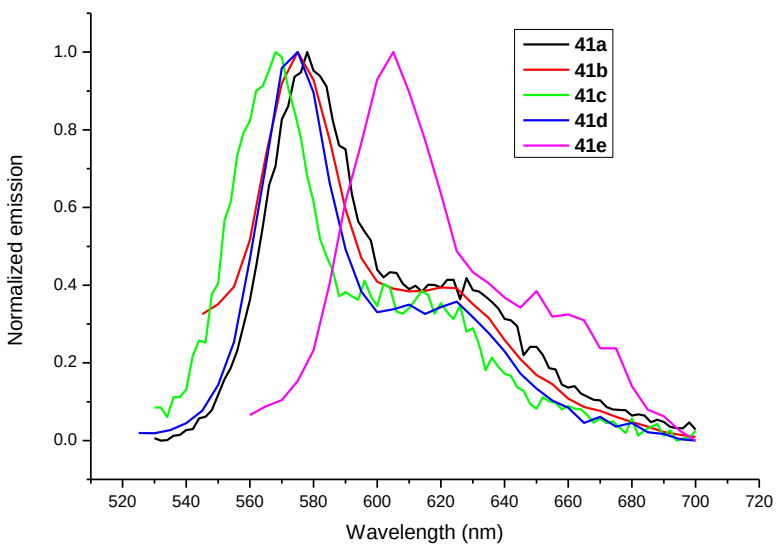

Figure 11. Phosphorescence of Pt complexes **41a-e**.

An immediately noticeable feature of the phosphorescence spectra is that the T_1 state of **41e** is considerably closer in energy to its S_0 state than is the case for the other Pt complexes. Thus, it can be anticipated that further tuning of the S_0-T_1 gap is possible by introducing other polycyclic aromatics in the 5-position of the oxazole.

The phosphorescence lifetimes of the complexes vary according to Table 4, from 26 μs to 366 μs. The reason for the rapid emptying of the T_1 state of **41c** compared to the other compounds is not known, but both such short lifetimes, and the longer ones, are known from our previous studies of other Pt complexes.[68] The lifetimes show that there is ample time for a population increase of the T_1 state for further absorption of light.

Along with the phosphorescence lifetimes, transient absorption spectra were obtained by pulse pumping a solution of the respective compound, and measuring after a short μs delay (Figure 12). Although the transient absorption spectra are somewhat noisy and difficult to fully interpret, they correlate with the OPL capabilities discussed below, and may be a valuable predictor for OPL performance.

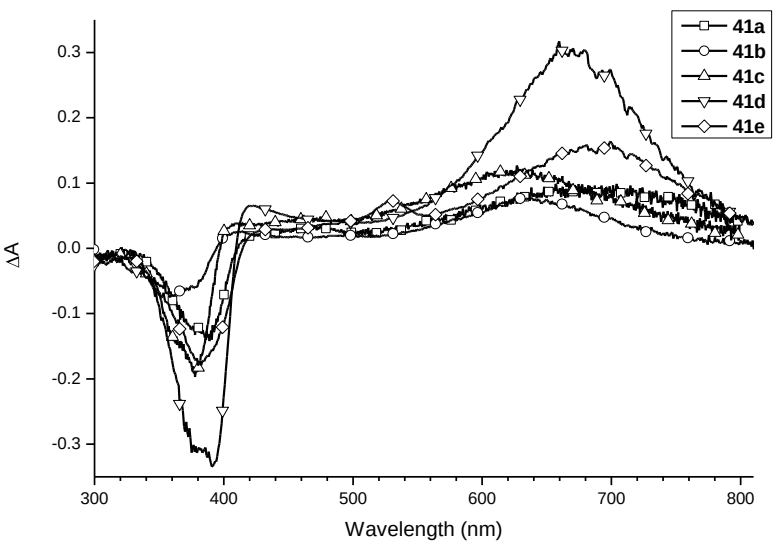

Figure 12. Transient absorption spectra of compounds **41a-e** (10 μM in THF).

Table 4. T_1 characterization of Pt complexes **41a-e.**

Compound	λ_{ph} (nm)	τ_{ph} (μs)	$\lambda_{max,T\text{-}T}$ (nm)	$\varepsilon_{T\text{-}T}{}^{a} \times 10^{-4}$ ($M^{-1}\,cm^{-1}$)
41a	578	181	700	2.9
41b	570	233	640	1.7
41c	568	26	630	4.1
41d	575	309	660	6.0
41e	605	366	700	3.4

[a]At $\lambda_{max,T\text{-}T}$. Adjusted to compensate for decay during the delay time.

The platinum complexes were tested for OPL performance using a pulsed laser setup, with results summarized in Figure 13. At 532 nm, **41a** and **41b** were clearly inferior to the others, with clamping energies near 10 μJ at higher fluences. This can be compared with the well-studied compound *trans*-$Pt(PBu_3)_2(C{\equiv}C\text{-}C_6H_4\text{-}C{\equiv}C\text{-}C_6H_5)_2$ that clamped near 7 μJ. On the other hand, compounds **41c-e** showed stronger limiting. When measuring at 600 nm, the output energy differences of the compounds were greater, spanning from approximately 25 to 3 μJ. The power limiting trend roughly followed that of 532 nm, with **41b** being an exception. Here, limiting was greatest with compound **41d**, with a clamping value just above 3 μJ.

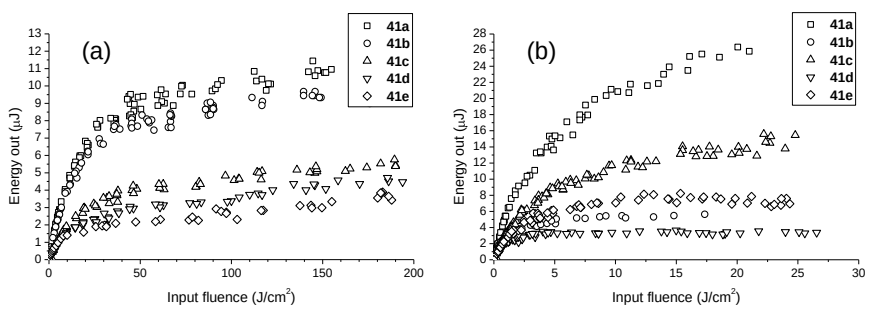

Figure 13. OPL performance of compounds **41a-e** (30 mM) at (a) 532 nm and (b) 600 nm.

The compounds were characterized by quantum chemistry calculations to gain further knowledge regarding their photophysical properties. The flexible PBu_3 ligands were again changed to PMe_3 in order to shorten the time for geometry optimizations. All ligands were optimized to a planar conformation, and all Pt complexes were, in the S_o state, found to have an energy minimum where the plane of the rings that are proximal to Pt is perpendicular to the Pt-P bond. Attempts to find an energy minimum where the referred dihedral angle is planar, by manually adjusting the bond angle, were not fruitful; however, the energy difference to such a conformation is in

the low kJ·mol^{-1} range and therefore a broad conformational distribution is expected at room temperature.

By restricting one of the ligands to be planar and the other to be perpendicular to the Pt-P bond and performing a geometry optimization, we noticed that the energies were slightly lower than the average of the planar and the perpendicular conformations. This, together with the large HOMO distribution of the compound (Figure 14) indicates that the ligands to some extent interact with each other over the Pt atom, even when perpendicular. The DFT calculation indicates that the π-orbitals of the planar ligand are conjugated, over the Pt atom, with the aligned π-orbitals of the alkyne on the other ligand. Again, as for the compounds in Paper I, the LUMO coefficient on platinum is large when one or more of the ligands are planar to the Pt-P bond.

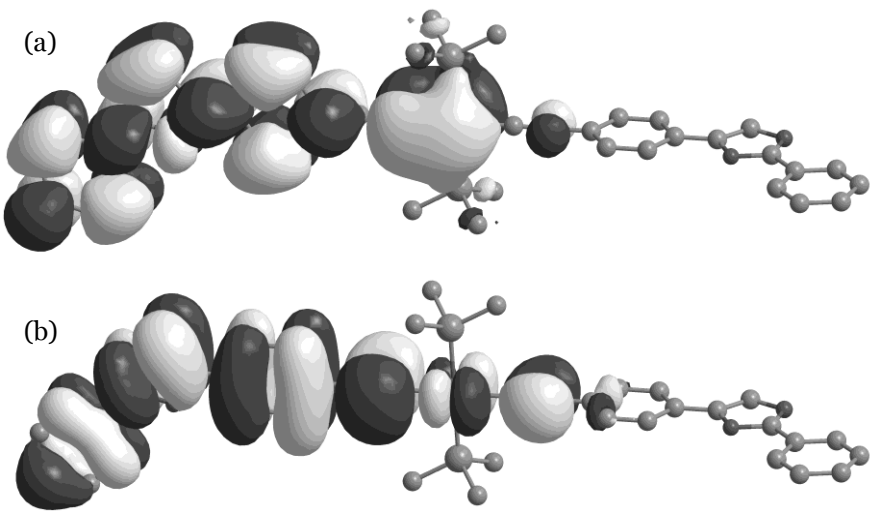

Figure 14. (a) LUMO and (b) HOMO of **41c**, having a pl-perp conformation.

Since the redshift upon coupling ligands **40a-e** to Pt to form Pt complexes **41a-e** differed between the compounds, we hypothesized that the reason for this might be a difference in ligand-Pt interaction strength, where a stronger interaction would induce a greater redshift, and investigated it using quantum chemical methods in two ways: by comparing the energy of the Pt complexes with their corresponding ligands, and by looking at the decrease of degeneracy of the lowest triplet states.

The gain in energy was obtained by subtracting twice the ligand energy from the Pt complex energy for each of the Pt complexes. The relative order

of the energies obtained indicate that electron deficient ligands **40a** and **40b** bind stronger to Pt than the other ligands.

In a complementary way to the first method, the energy splittings of the S_1 and S_2 states were compared. A weak interaction to Pt would imply that the two ligands would be degenerate, and the stronger the interaction, the greater the split of S_1 and S_2.[71] The results follow the same trend as when comparing the redshift and bond energies. Hence, in summary, it appears as electron deficient ligands bind stronger to platinum than electron rich ones. The reason for this is not known, but may be due to back donation of electrons from platinum to the LUMO of the ligand, which would be lowered by electron-withdrawing substituents, thus giving a more favorable interaction.

To understand whether the double peaks of the absorption spectrum of **41d** (Figure 9b, at 370 and 395 nm) were caused by two conformers, the electronic excitations of the structures in Figure 15 were calculated, using a solvent model to better model the experimental spectra. The SCF energies are virtually identical, indicating a 1:1 relationship between the conformations, as between the peaks in the experimental spectrum. But, in disagreement with our hypothesis, the excitation wavelengths are also identical, differing by a mere 0.1 nm. The double peak is therefore more likely to have some other cause, for example, excitation from S_0 to both the first and second vibronic state of S_1.

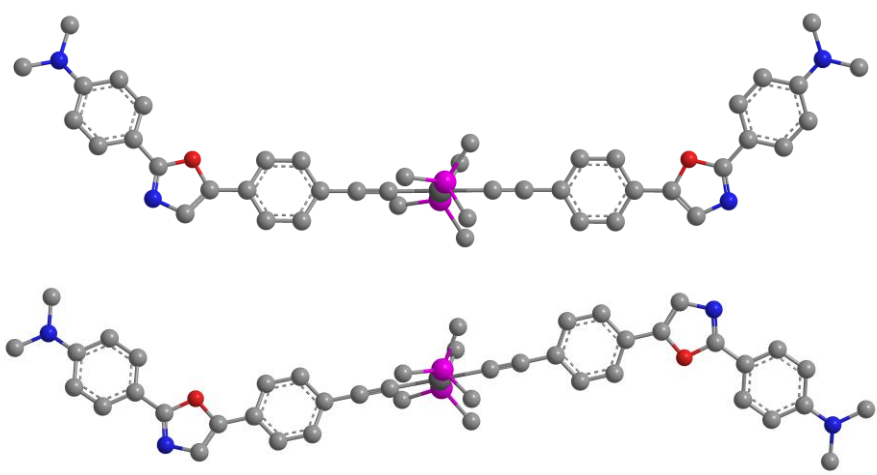

Figure 15. Examined possible conformers of **41d**.

In summary, the synthesized Pt complexes show promising OPL capabilities, but must be shielded from atmospheric oxygen to prevent decomposition.

The ligand-Pt interaction was shown to be modulated by the substituent of the aryl distal to Pt, with increased strength with the electron-withdrawing substituents. It is possible to use DFT methods to accurately predict S_1 and T_1 levels of similar compounds, given a small calibration set.

Paper III

With a main focus to find compounds for effective power limiting around 600 nm, the three compounds **48-50** (Chart 4) were investigated as interesting leads, and synthesized and tested with regard to OPL. Their triplet–triplet transitions were characterized using quantum chemistry calculations.

All compounds contain hydroxy groups at the ends of their rod-like structures. The reason for this was two-fold: the group can be further functionalized for inclusion in solid matrices,[72] and it can increase solubility in polar solvents for use in sol–gel glass preparation.

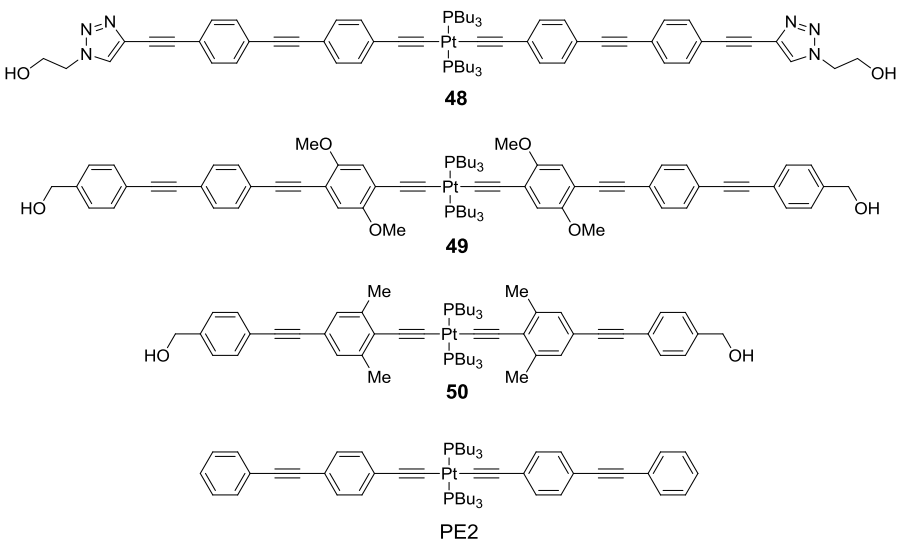

Chart 4. Chemical structures of platinum complexes **48-50** and PE2.

The synthesis, photophysical properties, and OPL capabilities of several triazoles connected to a platinum atom was reported earlier by Westlund et al.[73] The synthetic viability and stability of triazoles make such compounds attractive for many kinds of applications. However, synthetic reports of triazoles bearing an alkyne in the 4-position are scarce in the literature, with less than 20 publications at the time of this writing.[74] Most of those reports are from the mid-2000 and onward, after the discovery and development of the copper(I)-catalyzed azide-alkyne cycloaddition.[75-76] The synthesis of this moiety was accomplished by reacting materials **53** and **55** (Scheme 9) to give

compound **56**, which, after deprotection, gave terminal alkyne **57**. The coupling-deprotection strategy outlined in Paper I was followed here, but instead of a propargyl alcohol as the protecting group for the alkyne, TMS was used, having considerably milder requirements for deprotection. After the rod-like ligand was extended to three rings, coupling to platinum and deprotection gave desired compound **48**.

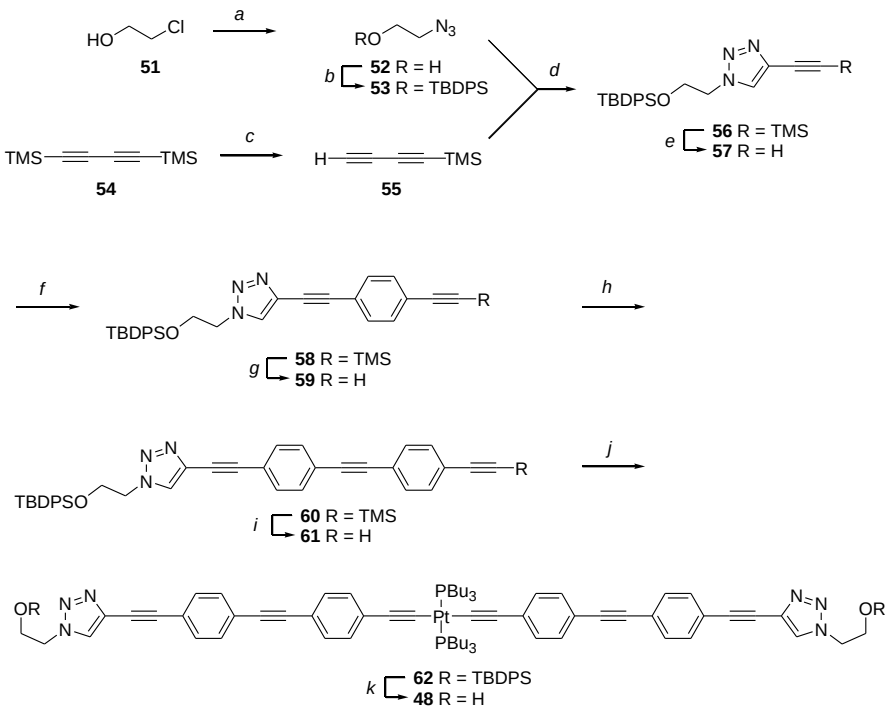

Scheme 9. Synthesis of compound **48**. *a*) NaN_3, H_2O, 87%; *b*) TBDPSCl, imidazol, CH_2Cl_2, 88%; *c*) MeLi-LiBr, Et_2O (n.q.); *d*) Na ascorbate, $CuSO_4$, MeOH/Et_2O/H_2O, 53%; *e*) K_2CO_3, MeOH, 88%; *f*) (4-iodophenylethynyl)-trimethylsilane, $PdCl_2(PPh_3)_2$, CuI, THF/Et_3N, 63%; *g*) As e, 84%; *h*) As f, 68%; *i*) As e, 87%; *j*) *trans*-$PtCl_2(PBu_3)_2$, CuI, THF/Et_3N, 54%; *k*) TBAF trihydrate, THF, 84%.

Compound **49** was synthesized according to Scheme 10 with the expectation that the methoxy groups of the phenylenes proximal to Pt would red-shift the triplet–triplet absorption band, and thus improve OPL at the red spectral area. The route was straight-forward and is described in further detail in the manuscript. It can however be noted that the bulky and fatty TIPS group facilitated column chromatography by making the intermediate compounds

more soluble; the low solubility of the longer arylethynyl chains can otherwise be troublesome.

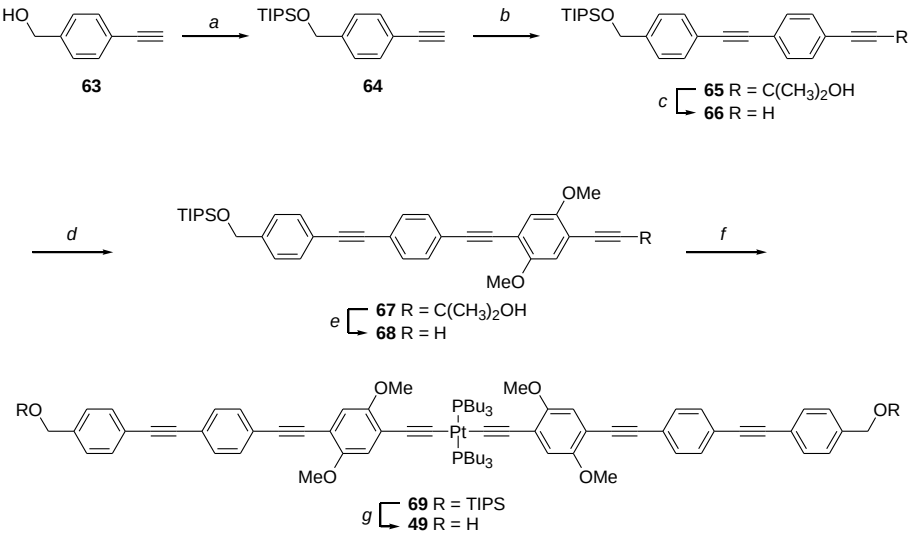

Scheme 10. Synthesis of compound **49**. *a*) TIPSCl, imidazol, CH_2Cl_2, 96%; *b*) **7**, $Pd(PPh_3)_2Cl_2$, CuI, THF/Et_3N, 99%; *c*) NaOH, toluene, 70%. *d*) **8**, see *b*. 85%; *e*) See *c*. 86%; *f*) *trans*-$PtCl_2(PBu_3)_2$, CuI, THF/Et_3N, 67%; *g*) TBAF trihydrate, THF, 96%.

The justification for investigating compound **50** is based on MO visualizations of the kind discussed in Paper I, where it was shown that the LUMO of compound **1** in an all-perpendicular conformation has a small coefficient on the platinum center. Hence, the ISC rate and OPL ability might be changed by changing the conformer ratio by the introduction of alkyls that would clash with the bulky phosphine ligands. A compound similar to **50** was investigated earlier in our laboratory, but was not tested with regard to OPL.[77]

The synthetic pathway, shown in Scheme 11, is somewhat different from the ones of, for example, **1**-**4** and **49**. Phenol **70** was iodinated to give **71**, then triflated to give pseudohalogen **72**. This allows for selective coupling because of the different reactivities of the 1- and 4-position. The more obvious way of coupling **64** to **71**, and subsequently triflating that product, failed due to decomposition of the product, but might also be a plausible route if other protecting groups are considered, assuming that was the problem. After coupling **63** to the iodine position, compound **73** was obtained. Under somewhat harsher coupling conditions and using TMS-acetylene as the coupling partner, a mixture of compounds **74** and **75** was obtained. Presumably the benzyl alcohol is silylated by the excess TMS-

acetylene, and the formed gaseous acetylene drives the C-Si ⇄ O-Si equilibrium forward. Fortunately, unexpected product **74** could be converted to **76** in excellent yield. After coupling to Pt, product **50** was obtained.

The same route, but starting from 2,6-diisopropylphenol instead of 2,6-dimethylphenol (**70**), was also attempted, but failed in the last step due to the lack of starting material reactivity. This may be due to the increased bulkiness of the isopropyl groups, but the failed reaction was not investigated further due to time constraints.

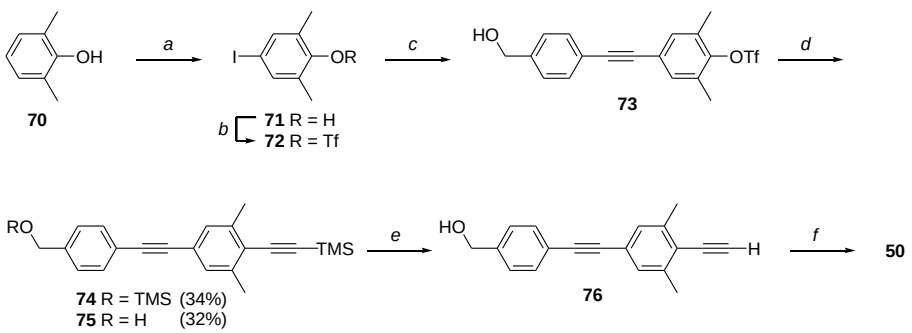

Scheme 11. Synthesis of compound **50**. *a*) NIS, TsOH, $CHCl_3$, 90%; b) Tf_2O, pyridine, CH_2Cl_2, 99%; c) **63**, $Pd(PPh_3)_2Cl_2$, CuI, THF/Et_3N, 66%; d) $Pd(PPh_3)_2Cl_2$, CuI, LiCl, TMS-acetylene, DMF/Et_2NH, 34%/32% resp.; e) K_2CO_3, MeOH, quant.; f) *trans*-$PtCl_2(PBu_3)_2$, CuI, THF/Et_3N, 54%.

After obtaining the desired compounds, they were subjected to OPL measurements at 532 and 600 nm, with the main results shown in Figure 16. Triazole-containing compound **48** showed promising results, with good clamping at both 532 and 600 nm. Compound **49**, bearing methoxy substituents, was found to be even better, with clamping values lower than 3 μJ at both measured wavelengths, which is better than for **1-4,** and approximately equal to that of **41d**. The geometry-constrained compound **50**, however, showed relatively low power attenuation, with high output energy. Compared to PE2 (shown in Chart 4, with hydrogens in place of the methyls), compound **50** is approximately equal in power limiting at 532 nm, and slightly inferior at 600 nm. We speculated that the reason for the difference in limiting might be a difference in the triplet–triplet absorption spectrum induced by geometry changes in the T_1 state, and used quantum chemical methods to calculate the electronic transitions.

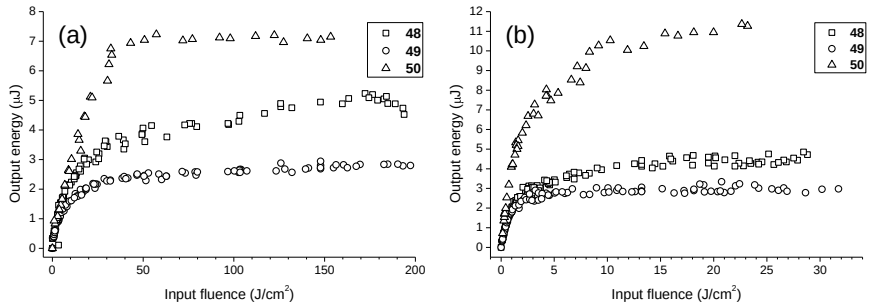

Figure 16. OPL of compounds **48-50** (30 mM in THF) at (a) 532 nm and (b) 600 nm.

First, the geometries of structures **48-50**, simplified with a methyl in place of the pendant hydroxyalkyl group and with PMe_3 instead of PBu_3, were optimized in the T_1 state. Immediately noticeable was the fact that neither of the alkynylaryl ligands ring of **49** (and **50**) were aligned with the Pt-P bond, as is otherwise common in the triplet state of similar structures, and was the case for **48**. This is in agreement with the hypothesis that the conformational distribution of **49** in solution is shifted towards the ligand ring being perpendicular to the Pt-P bond.

Following the geometry optimizations, the electronic excitations from T_1 were obtained by TDDFT methods with the functionals B3LYP and CAM-B3LYP, and are summarized in Table 5. There is a clear discrepancy in the B3LYP-calculated wavelength corresponding to the S_0–S_1 transition between **50** and PE2. Although not yet fully investigated, it is unlikely that the wavelength difference is due to electronic differences between methyls and hydrogens, and, instead, it may be caused by the geometry difference.

The validity of the calculations, and the difference between B3LYP and CAM-B3LYP is further explored in Paper V. In brief, we show in that manuscript that B3LYP gave better predictions for λ_{max} than did CAM-B3LYP, though the experimental triplet–triplet absorption spectra are usually very broad and should be interpreted with caution. Here, we note that the correlation between the CAM-B3LYP excitation wavelengths and oscillator strengths, and the OPL of the synthesized compounds is striking.

Table 5. Calculated excitations with the largest oscillator strengths.

	Wavelength [Oscillator strength]	
Compound	B3LYP	CAM-B3LYP
48	695 [1.30]	577 [3.08]
	643 [1.79]	502 [0.67]
49	706 [0.67]	580 [2.88]
	657 [1.40]	527 [0.46]
	618 [0.74]	
50	524 [1.44]	471 [1.57]
PE2	602 [1.61]	497 [1.86]

To summarize, three novel structures were synthesized and tested for OPL. Especially one of them, compound **49**, shows promising results with its low clamping levels. The compounds' triplet–triplet absorption was characterized *in silico* and was found to correlate with the experimental OPL.

Paper IV

This paper was motivated by a desire to create solid matrices that contain chromophores of the type described in this thesis. Previous studies using PMMA have shown promising results,[78] but there is a need for stable glass-like matrices that are able to absorb and dissipate the heat generated by the absorption of strong light. Earlier work has shown that it is possible to graft silicon-derivatized chromophores into silica matrices.[72, 79] Unfortunately, the derivatives are unstable, and cumbersome to purify. In addition, it has previously been difficult to create materials with high loadings of chromophores. The results presented in this paper, investigating silica materials, alleviates some of these problems.

Silica glass, as found in window panes and everyday objects, is manufactured by melting silica particles, and shaping the viscuous melt. This process is not possible to use when there is a desire to incorporate sensitive organic molecules into the glass because of the high temperatures needed. Instead, the glass may be formed chemically by the hydrolysis of an alkyl silicate or similar species, followed by condensation.[80] This is called a "sol–gel" process, referring to a *sol*ution becoming a *gel*.

There are two main classes of hybrid sol–gel materials. In class I, the compound of interest is dispersed in the matrix without strong bonding, analogous to a solution. In class II, there is strong bonding, such as covalent bonding, between the compound and the matrix.

Compounds **77**-**79** (Chart 5) were synthesized using the strategy outlined in Paper I, and the synthesis is not further expounded upon here.

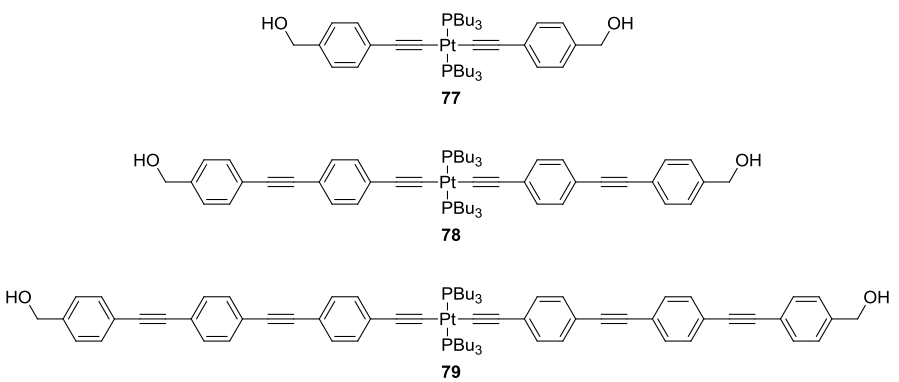

Chart 5. Chemical structures of compounds **77**-**79**.

The sol–gels were prepared in the laboratory of our collaborators by first hydrolyzing an alkoxysilane precursor; example precursors are shown in

Chart 6. In this work, several additional precursors than those shown were used, with other organic groups attached to the silicon atom. After removal of the resulting alcohol product and water, the sol (*i.e.*, the unpolymerized solution) is stable and can be stored cold for months. Solutions of compounds **77-79** were prepared and mixed with different sols. Then, in a crucial step, condensation was induced by the addition of an amine base; here APTES was used. After the addition, the sol quickly gelates and traps the chromophore, preventing aggregation should it be a problem.

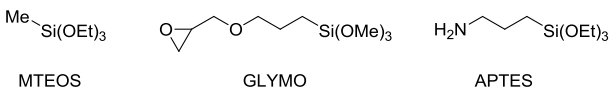

Chart 6. Chemical structures of example sol–gel precursors MTEOS and GLYMO, and condensation catalyst APTES.

The microstructure of the gel can be controlled by the choice of precursor. This was shown by using positron annihilation lifetime spectroscopy, where the lifetime of a formed positron–electron adduct, termed positronium, is dependent on pore size. By comparing the positronium lifetimes of an MTEOS glass and an MTEOS–GLYMO 80:20 mixed glass, it was found that the latter glass lacked the largest pores seen in the MTEOS glass.

The larger pores in the MTEOS glass was also qualitatively demonstrated by observing the phosphorescence from the materials when they were irradiated with UV light. The pore size allowed diffusion of atmospheric oxygen into the material, quenching the phosphorescence, while the MTEOS–GLYMO mixed glass, having smaller pores, showed strong phosphorescence. This observation can be important in the incorporation of oxygen sensitive compounds, such as **41a-e**.

The OPL abilities of the compounds in an MTEOS matrix was examined and was found to be approximately equal to the solution OPL, showing that the properties of the compounds are preserved during the sol condensation.

Paper V

The chemical synthesis of a compound can be time-consuming and costly. It is unfortunately often the only way to obtain reliable information regarding physical properties. In this work, we investigate the possibility to use *in silico* methods to gain knowledge about triplet–triplet absorption. A method for pre-selecting compounds based on methods that are faster and easier than synthesis would be beneficial to research in general. Here, two different methods to predict the triplet–triplet absorption of compounds **41a-e** (Scheme 6, page 18) and compound PE2 were explored. In the same way as described earlier in this thesis, the structures were simplified for the calculations by exchanging the PBu_3 groups for PMe_3.

The use of *in silico* methods to predict triplet–triplet excitation energies for organometallic species are, compared to singlet–singlet excitations, relatively rare, but a few reports are available.[81-82] In a seminal paper by Nguyen *et al.*,[81] triplet absorption spectra of several organic and organometallic dyes were compared with calculated triplet–triplet excitations. A good coincidence of excitations was found when using the B3LYP functional, and, in fact, the mean error was found to be smaller for T_1–T_n excitations than for S_0-S_n excitations for the test set used.

The structures for **41a-e**, which had been geometry optimized in their lowest triplet state for Paper II using the B3LYP functional, were subjected to unrestricted TDDFT calculations with both the B3LYP and the CAM-B3LYP functional from their respective optimized T_1 electronic structure. Additionally, a method using restricted DFT was used, where the electronic structure is optimized in the S_0 state, and T_1–T_n excitation energies and oscillator strengths are obtained by a second-order response function.[83] For the restricted method, functional CAM-B3LYP was used. Although the effect of the basis set has been shown to be small,[81] a relatively large basis was used to maintain consistency with the calculations in Paper II.

A comparison indicate that all calculated excitation energies, for the transition with the largest oscillator strength, are in remarkable agreement with the energy gap corresponding to the experimental λ_{max} (Table 6, with transient absorption spectra shown in Figure 12 on page 23). For this small set of molecules, unrestricted B3LYP gives the prediction with the smallest RMSE of 0.15 eV and a maximum error of 0.22 eV for compound **41c**. Unrestricted CAM-B3LYP, commonly giving smaller errors for charge-transfer excitations,[84] here gave excitation energy gaps larger than for B3LYP, with the slightly higher RMSE of 0.25 eV. The functionals closely follow the same trend between for **41a-e**, though the CAM-B3LYP functional gives a higher energy value for PE2, compared to **41e-e**, than does B3LYP.

Table 6. Experimental and calculated T–T excitations.[a]

Compd	$\Delta E_{T\text{-}T}$ [b]	UB3LYP [c]	UCAM-B3LYP [c]	RCAM-B3LYP [c]
41a	1.77 [2.9]	1.71 [1.05]	1.97 [1.17]	2.25 [0.56]
41b	1.94 [1.7]	1.73 [0.90]	2.01 [1.07]	2.15 [0.16]
41c	1.97 [4.1]	1.75 [0.78]	2.03 [0.94]	2.22 [0.38]
41d	1.88 [6.0]	1.73 [0.63]	2.03 [0.99]	2.13 [0.20]
41e	1.77 [3.4]	1.85 [0.79]	2.17 [0.98]	2.11 [0.12]
PE2	2.14 [4.5]	2.06 [1.61]	2.50 [1.86]	2.74 [0.42]

[a] Energy gaps in eV. [b] Gap ±0.02 eV. $\varepsilon_{T\text{-}T} \times 10^{-4}$ in brackets. [c] Oscillator strength in brackets.

Using the restricted formalism, the calculated excitation energies again follow the experimental ones, and show good agreement with the unrestricted energies, with an RMSE of 0.38 eV. This must be considered remarkable given the advanced level of the calculation, where neither the ground state electronic structure nor the excited state electronic structure are optimized to a triplet state.

The oscillator strengths reported by the unrestricted methods give consistent values; however, this is not the case for the restricted method, which would appear difficult to use for predicting strong triplet–triplet absorbing compounds.

The RMSE values should be used with caution, because the calculated transition may not correspond to λ_{max} of the broad experimental spectrum, and, hence, CAM-B3LYP or some other functional may give better predictions than B3LYP after using a calibration set.

In Paper II, it was shown that the experimental S_0–S_1 and S_0–T_1 energy gaps for compounds **41a-e** gave good correlations with calculated gaps. However, this was not the case for T_1–T_n in the present work. As visualized in Figure 17, the calculated excitation energy of compound **41e** is overestimated, and the calculated energies in general have a smaller span than the experimental ones. The spin-restricted method gives a somewhat better correlation to the experimental energies, with an R^2 value at 0.62, than the unrestricted methods with R^2 values near 0.45 (linear regression not shown).

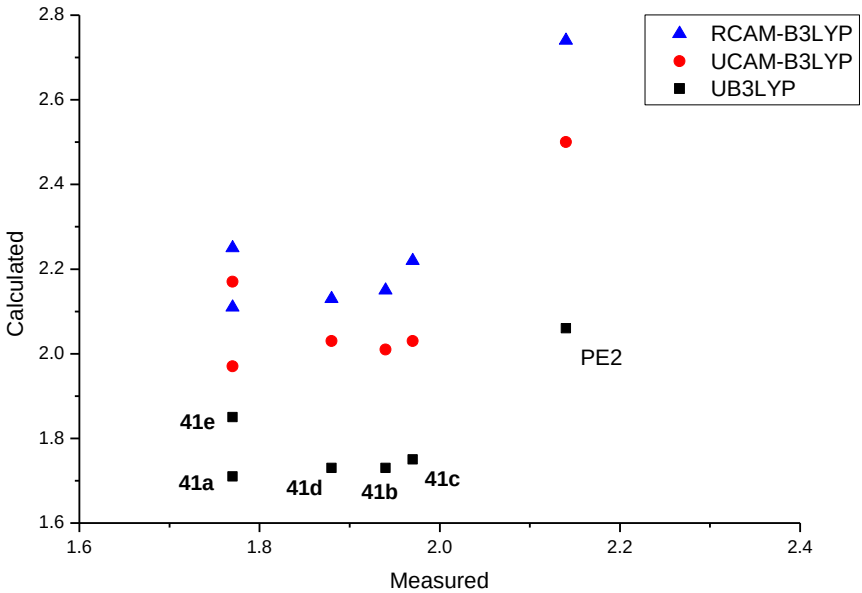

Figure 17. Calculated T–T excitation energies versus measured λ_{max} of **41a-e** and PE2.

Concluding remarks

In our quest for new, strongly active OPL molecules, we have made scientific contributions in several ways. From basic research, trying to understand and predict the processes that occur in these molecules, *via* rational design and synthesis of chromophores, to the production of active materials. Still, after my five years in the project, I feel that I have barely begun to scratch the surface of what could be done.

Some of the more interesting areas to study further would, in my opinion, be triplet–triplet excitation calculations. More recent functionals often compare favorably to the somewhat routine choices, and a side-by-side evaluation would be helpful in future calculations.

Since the triplet exciton, for the compounds studied in this work, is localized to one ligand, an *in silico* study comparing Pt complexes and their corresponding ligands would show if the computing time could be greatly reduced by performing the calculation on the ligand only.

Conformational restriction of ligands, but in a “planar” fashion as opposed to the here studied “perpendicular” fashion, could also be interesting, both from synthetical and photophysical points of view.

Although not a major part of my research, I find the sol–gel process to be intriguing — not only for OPL materials — but with good imagination and multidisciplinary collaborations, many novel functional materials could possibly be made.

With that, I wish good luck to present and future collaborators on the project!

Acknowledgements

Min handledare **Bertil** för all hjälp jag fått med mitt arbete här;

min biträdande handledare **Dan** för intressanta diskussioner;

Marcus Carlsson för hans tidigare arbete på projektet och för all hjälp jag fick när jag började;

Pål Ellingsen, **Eirik Glimsdal** och **Mikael Lindgren** i Trondheim för fotofysikalisk expertis;

Cesar Lopes med grupp på FOI i Linköping för OPL-mätningar;

Stephane Parola med grupp i Lyon för glastillverkning;

Patrick Norman för diskussioner kring kvantkemiska beräkningar;

Michael Sharp för språkgranskning;

instrumentell hjälp från **Radek**, **Therese** och **Sergey**;

Kempestiftelsen för finansiellt stöd;

alla kontors- och labbkamrater jag haft genom åren och övriga jag snackat extra mycket ovidkommande saker med (även lite kemi), särskilt **Sofie**, **Mackan**, **Christoffer, John**, **Andreas, Marcus W**, **Sara** och **Morakot**;

exjobbare och studenter jag har fått öva handledarskap och pedagogik på;

alla mina arbetskamrater som gjort jobbet till ett fantastiskt roligt ställe att gå till;

och sist, men inte minst, **Karin** och min familj;

från botten av mitt hjärta: tack!

References

1. Kasha, M., Characterization of electronic transitions in complex molecules. *Discuss. Faraday. Soc.* **1950,** *9*, 14-19.

2. Itoh, T., Fluorescence and Phosphorescence from Higher Excited States of Organic Molecules. *Chem. Rev.* **2012,** *112* (8), 4541-68.

3. Göppert-Mayer, M., Über Elementarakte mit zwei Quantensprüngen. *Ann. Phys.* **1931,** *401* (3), 273-294.

4. Kaiser, W.; Garrett, C. G. B., Two-Photon Excitation in CaF_2: Eu^{2+}. *Phys. Rev. Lett.* **1961,** *7* (6), 229-231.

5. So, P. T. C.; Dong, C. Y.; Masters, B. R.; Berland, K. M., Two-photon excitation fluorescence microscopy. *Annu. Rev. Biomed. Eng.* **2000,** *2* (1), 399-429.

6. Helmchen, F.; Denk, W., Deep tissue two-photon microscopy. *Nat. Methods* **2005,** *2* (12), 932-940.

7. Cumpston, B. H.; Ananthavel, S. P.; Barlow, S.; Dyer, D. L.; Ehrlich, J. E.; Erskine, L. L.; Heikal, A. A.; Kuebler, S. M.; Lee, I. Y. S.; McCord-Maughon, D.; Qin, J. Q.; Rockel, H.; Rumi, M.; Wu, X. L.; Marder, S. R.; Perry, J. W., Two-photon polymerization initiators for three-dimensional optical data storage and microfabrication. *Nature* **1999,** *398* (6722), 51-54.

8. Nguyen, L. H.; Straub, M.; Gu, M., Acrylate-Based Photopolymer for Two-Photon Microfabrication and Photonic Applications. *Adv. Funct. Mater.* **2005,** *15* (2), 209-216.

9. LaFratta, C. N.; Fourkas, J. T.; Baldacchini, T.; Farrer, R. A., Multiphoton Fabrication. *Angew. Chem., Int. Ed.* **2007,** *46* (33), 6238-6258.

10. Fisher, W. G.; Partridge, W. P.; Dees, C.; Wachter, E. A., Simultaneous Two-Photon Activation of Type-I Photodynamic Therapy Agents. *Photochem. Photobiol.* **1997,** *66* (2), 141-155.

11. Starkey, J. R.; Rebane, A. K.; Drobizhev, M. A.; Meng, F.; Gong, A.; Elliott, A.; McInnerney, K.; Spangler, C. W., New Two-Photon Activated

Photodynamic Therapy Sensitizers Induce Xenograft Tumor Regressions after Near-IR Laser Treatment through the Body of the Host Mouse. *Clin. Cancer Res.* **2008,** *14* (20), 6564-6573.

12. Qian, J.; Wang, D.; Cai, F.; Zhan, Q.; Wang, Y.; He, S., Photosensitizer encapsulated organically modified silica nanoparticles for direct two-photon photodynamic therapy and In Vivo functional imaging. *Biomaterials* **2012,** *33* (19), 4851-4860.

13. Morel, Y.; Irimia, A.; Najechalski, P.; Kervella, Y.; Stephan, O.; Baldeck, P. L.; Andraud, C., Two-photon absorption and optical power limiting of bifluorene molecule. *J. Chem. Phys.* **2001,** *114* (12), 5391.

14. Charlot, M.; Izard, N.; Mongin, O.; Riehl, D.; Blanchard-Desce, M., Optical limiting with soluble two-photon absorbing quadrupoles: Structure–property relationships. *Chem. Phys. Lett.* **2006,** *417* (4–6), 297-302.

15. Belfield, K. D.; Bondar, M. V.; Hernandez, F. E.; Przhonska, O. V., Photophysical Characterization, Two-Photon Absorption and Optical Power Limiting of Two Fluorenylperylene Diimides. *J. Phys. Chem. C* **2008,** *112* (14), 5618-5622.

16. McKay, T. J.; Staromlynska, J.; Wilson, P.; Davy, J., Nonlinear luminescence spectroscopy in a Pt:ethynyl compound. *J. Appl. Phys.* **1999,** *85* (3), 1337-1341.

17. Turro, N. J., *Modem Molecular Photochemistry*. Benjamin/Cummings Menlo Park, CA, 1978.

18. El-Sayed, M. A., Triplet state. Its radiative and nonradiative properties. *Acc. Chem. Res.* **1968,** *1* (1), 8-16.

19. Wray, J. E.; Liu, K. C., Optical power limiting of fullerenes. *Appl. Phys. Lett.* **1994,** *64* (21), 2785.

20. Perry, J. W.; Mansour, K.; Marder, S. R.; Perry, K. J.; Alvarez, D., Jr.; Choong, I., Enhanced reverse saturable absorption and optical limiting in heavy-atom-substituted phthalocyanines. *Opt. Lett.* **1994,** *19* (9), 625-7.

21. Perry, J. W.; Mansour, K.; Lee, I. Y. S.; Wu, X. L.; Bedworth, P. V.; Chen, C. T.; Ng, D.; Marder, S. R.; Miles, P.; Wada, T.; Tian, M.; Sasabe, H., Organic Optical Limiter with a Strong Nonlinear Absorptive Response. *Science* **1996,** *273* (5281), 1533-1536.

22. Dini, D.; Barthel, M.; Hanack, M., Phthalocyanines as active materials for optical limiting. *Eur. J. Org. Chem.* **2001,** *2001* (20), 3759-3769.

23. Staromlynska, J.; McKay, T. J.; Bolger, J. A.; Davy, J. R., Evidence for broadband optical limiting in a Pt : ethynyl compound. *J. Opt. Soc. Am. B: Opt. Phys.* **1998,** *15* (6), 1731-1736.

24. McKay, T. J.; Bolger, J. A.; Staromlynska, J.; Davy, J. R., Linear and nonlinear optical properties of platinum-ethynyl. *J. Chem. Phys.* **1998,** *108* (13), 5537-5541.

25. Staromlynska, J.; McKay, T. J.; Wilson, P., Broadband optical limiting based on excited state absorption in Pt:ethynyl. *J. Appl. Phys.* **2000,** *88* (4), 1726-1732.

26. Zhou, G. J.; Wong, W. Y., Organometallic acetylides of Pt(II), Au(I) and Hg(II) as new generation optical power limiting materials. *Chem. Soc. Rev.* **2011,** *40* (5), 2541-66.

27. Chatt, J.; Shaw, B. L., 808. Alkyls and aryls of transition metals. Part II. Platinum(II) derivatives. *J. Chem. Soc.* **1959**, 4020-4033.

28. D'Amato, R.; Furlani, A.; Colapietro, M.; Portalone, G.; Casalboni, M.; Falconieri, M.; Russo, M. V., Synthesis, characterisation and optical properties of symmetrical and unsymmetrical Pt(II) and Pd(II) bis-acetylides. Crystal structure of trans- Pt(PPh3)(2)(C C-C6H5)(C C-C6H4NO2). *J. Organomet. Chem.* **2001,** *627* (1), 13-22.

29. Hissler, M.; Connick, W. B.; Geiger, D. K.; McGarrah, J. E.; Lipa, D.; Lachicotte, R. J.; Eisenberg, R., Platinum diimine bis(acetylide) complexes: Synthesis, characterization, and luminescence properties. *Inorg. Chem.* **2000,** *39* (3), 447-457.

30. Yam, V. W.-W.; Wong, K. M.-C.; Zhu, N., Luminescent platinum(II) terpyridyl-capped carbon-rich molecular rods-an extension from molecular- to nanometer-scale dimensions. *Angew. Chem., Int. Ed.* **2003,** *42* (12), 1400-1403.

31. Zhao, M. T.; Cui, Y. P.; Samoc, M.; Prasad, P. N.; Unroe, M. R.; Reinhardt, B. A., Influence of 2-Photon Absorption on 3rd-Order Nonlinear Optical Processes as Studied by Degenerate 4-Wave-Mixing - the Study of Soluble Didecyloxy Substituted Polyphenyls. *J. Chem. Phys.* **1991,** *95* (6), 3991-4001.

32. Porter, P. L.; Guha, S.; Kang, K.; Frazier, C. C., Effects of structural variations of platinum and palladium polyynes on third-order nonlinearity. *Polymer* **1991,** *32* (10), 1756-60.

33. Grim, S. O.; Keiter, R. L.; McFarlane, W., A phosphorus-31 nuclear magnetic resonance study of tertiary phosphine complexes of platinum(II). *Inorg. Chem.* **1967,** *6*, 1133-1137.

34. Brown, D. J.; Ghosh, P. B., The spectra, ionization, and deuteriation of oxazoles and related compounds. *J. Chem. Soc. B* **1969**, 270-276.

35. Cramer, C. J., *Essentials of Computational Chemistry: Theories and Models*. 2nd ed.; John Wiley & Sons: 2004.

36. Becke, A. D., Density-Functional Thermochemistry .3. The Role of Exact Exchange. *J. Chem. Phys.* **1993,** *98* (7), 5648-5652.

37. Lee, C.; Yang, W.; Parr, R. G., Development of the Colle-Salvetti correlation-energy formula into a functional of the electron density. *Phys. Rev. B* **1988,** *37* (2), 785-789.

38. Becke, A. D., Density-functional exchange-energy approximation with correct asymptotic behavior. *Phys. Rev. A* **1988,** *38* (6), 3098-3100.

39. Perdew, J. P.; Burke, K.; Ernzerhof, M., Generalized Gradient Approximation Made Simple. *Phys. Rev. Lett.* **1996,** *77* (18), 3865-3868.

40. Adamo, C.; Barone, V., Exchange functionals with improved long-range behavior and adiabatic connection methods without adjustable parameters: The mPW and mPW1PW models. *J. Chem. Phys.* **1998,** *108* (2), 664-675.

41. Perdew, J. P.; Chevary, J. A.; Vosko, S. H.; Jackson, K. A.; Pederson, M. R.; Singh, D. J.; Fiolhais, C., Atoms, molecules, solids, and surfaces: Applications of the generalized gradient approximation for exchange and correlation. *Phys. Rev. B* **1992,** *46* (11), 6671-6687.

42. Zhao, Y.; Truhlar, D., The M06 suite of density functionals for main group thermochemistry, thermochemical kinetics, noncovalent interactions, excited states, and transition elements: two new functionals and systematic testing of four M06-class functionals and 12 other functionals. *Theor. Chem. Acc.* **2008,** *120* (1-3), 215-241.

43. Yanai, T.; Tew, D. P.; Handy, N. C., A new hybrid exchange-correlation functional using the Coulomb-attenuating method (CAM-B3LYP). *Chem. Phys. Lett.* **2004,** *393* (1-3), 51-57.

44. Anslyn, E. V.; Dougherty, D. A., *Modern Physical Organic Chemistry*. University Science: 2006.

45. Koch, W.; Holthausen, M. C., *A Chemist's Guide to Density Functional Theory*. Second ed.; Wiley-VCH: Weinheim, 2001.

46. Lindgren, M.; Minaev, B.; Glimsdal, E.; Vestberg, R.; Westlund, R.; Malmstrom, E., Electronic states and phosphorescence of dendron functionalized platinum(II) acetylides. *J. Lumin.* **2007,** *124* (2), 302-310.

47. Ozimiński, W. P.; Garnuszek, P.; Bednarek, E.; Dobrowolski, J. C., The platinum complexes with histamine: Pt(II)(Hist)Cl2, Pt(II)(Iodo-Hist)Cl2 and Pt(IV)(Hist)2Cl2. *Inorg. Chim. Acta* **2007,** *360* (6), 1902-1914.

48. Zhang, G.; Musgrave, C. B., Comparison of DFT Methods for Molecular Orbital Eigenvalue Calculations. *J. Phys. Chem. A* **2007,** *111* (8), 1554-1561.

49. Liu, R.; Zhou, D.; Azenkeng, A.; Li, Z.; Li, Y.; Glusac, K. D.; Sun, W., Nonlinear Absorbing Platinum(II) Diimine Complexes: Synthesis, Photophysics, and Reverse Saturable Absorption. *Chem. Eur. J.* **2012,** *18* (36), 11440-11448.

50. Carmichael, I.; Hug, G. L., Triplet--Triplet Absorption Spectra of Organic Molecules in Condensed Phases. *J. Phys. Chem. Ref. Data* **1986,** *15* (1), 1-250.

51. Rogers, J. E.; Hall, B. C.; Hufnagle, D. C.; Slagle, J. E.; Ault, A. P.; McLean, D. G.; Fleitz, P. A.; Cooper, T. M., Effect of platinum on the photophysical properties of a series of phenyl-ethynyl oligomers. *J. Chem. Phys.* **2005,** *122* (21), 214708

52. Robinson, R., CCXXXII.-A new synthesis of oxazole derivatives. *J. Chem. Soc., Trans.* **1909,** *95*, 2167-2174.

53. Gabriel, S., Eine Synthese von Oxazolen und Thiazolen. I. *Chem. Ber.* **1910,** *43* (1), 134-138.

54. Staudinger, H.; Meyer, J., Über neue organische Phosphorverbindungen III. Phosphinmethylenderivate und Phosphinimine. *Helv. Chim. Acta* **1919,** *2* (1), 635-646.

55. Heathcock, C. H.; Smith, S. C., Synthesis and Biological Activity Of Unsymmetrical Bis-Steroidal Pyrazines Related to the Cytotoxic Marine Natural Product Cephalostatin 1. *J. Org. Chem.* **1994,** *59* (22), 6828-6839.

56. Nudelman, A.; Bechor, Y.; Falb, E.; Fischer, B.; Wexler, B. A.; Nudelman, A., Acetyl Chloride-Methanol as a Convenient Reagent for: A) Quantitative Formation of Amine Hydrochlorides B) Carboxylate Ester Formation C) Mild Removal of N-t-Boc-Protective Group. *Synth. Commun.* **1998,** *28* (3), 471-474.

57. Schotten, C., Ueber die Oxydation des Piperidins. *Chem. Ber.* **1884,** *17* (2), 2544-2547.

58. Baumann, E., Ueber eine einfache Methode der Darstellung von Benzoësäureäthern. *Chem. Ber.* **1886,** *19* (2), 3218-3222.

59. Eschweiler, W., Ersatz von an Stickstoff gebundenen Wasserstoffatomen durch die Methylgruppe mit Hülfe von Formaldehyd. *Chem. Ber.* **1905,** *38* (1), 880-882.

60. Clarke, H. T.; Gillespie, H. B.; Weisshaus, S. Z., The Action of Formaldehyde on Amines and Amino Acids. *J. Am. Chem. Soc.* **1933,** *55* (11), 4571-4587.

61. Borch, R. F.; Hassid, A. I., New method for the methylation of amines. *J. Org. Chem.* **1972,** *37* (10), 1673-1674.

62. Ho, T.-L., Dealkylation of Quaternary Ammonium Salts with 1,4-Diazabicyclo[2.2.2]octane. *Synthesis* **1972,** *1972* (12), 702,702.

63. Sonogashira, K.; Yatake, T.; Tohda, Y.; Takahashi, S.; Hagihara, N., Novel preparation of s-alkynyl complexes of transition metals by copper(I) iodide-catalyzed dehydrohalogenation. *J. Chem. Soc., Chem. Commun.* **1977,** (9), 291-2.

64. Sonogashira, K.; Fujikura, Y.; Yatake, T.; Toyoshima, N.; Takahashi, S.; Hagihara, N., Syntheses and properties of cis- and trans-dialkynyl complexes of platinum(II). *J. Organomet. Chem.* **1978,** *145* (1), 101-8.

65. Wasserman, H. H.; Floyd, M. B., The oxidation of heterocyclic systems by molecular oxygen—IV : The photosensitized autoxidation of oxazoles. *Tetrahedron* **1966,** *22 (Supplement 7)*, 441-448.

66. George, M. V.; Bhat, V., Photooxygenations of nitrogen heterocycles. *Chem. Rev.* **1979,** *79* (5), 447-478.

67. Gollnick, K.; Koegler, S., (4+2)-cycloaddition of singlet oxygen to oxazoles formation of oxazole endoperoxides. *Tetrahedron Lett.* **1988,** *29* (9), 1003-1006.

68. Glimsdal, E.; Carlsson, M.; Kindahl, T.; Lindgren, M.; Lopes, C.; Eliasson, B., Luminescence, Singlet Oxygen Production, and Optical Power Limiting of Some Diacetylide Platinum(II) Diphosphine Complexes. *J. Phys. Chem. A* **2010,** *114* (10), 3431-3442.

69. Oskouei, A. A.; Bräm, O.; Cannizzo, A.; van Mourik, F.; Tortschanoff, A.; Chergui, M., Ultrafast UV photon echo peak shift and fluorescence up conversion studies of non-polar solvation dynamics. *Chem. Phys.* **2008,** *350* (1–3), 104-110.

70. Montalti, M.; Credi, A.; Luca, P.; Gandolfi, M. T., *Handbook of Photochemistry*. CRC/Taylor & Francis: Boca Raton, 2006.

71. Norman, P.; Jensen, H. J. A., Phosphorescence parameters for platinum (II) organometallic chromophores: A study at the non-collinear four-component Kohn–Sham level of theory. *Chem. Phys. Lett.* **2012,** *531* (0), 229-235.

72. Zieba, R.; Desroches, C.; Chaput, F.; Carlsson, M.; Eliasson, B.; Lopes, C.; Lindgren, M.; Parola, S., Preparation of Functional Hybrid Glass Material from Platinum (II) Complexes for Broadband Nonlinear Absorption of Light. *Adv. Funct. Mater.* **2009,** *19* (2), 235-241.

73. Westlund, R.; Glimsdal, E.; Lindgren, M.; Vestberg, R.; Hawker, C.; Lopes, C.; Malmstrom, E., Click chemistry for photonic applications: triazole-functionalized platinum(II) acetylides for optical power limiting. *J. Mater. Chem.* **2008,** *18* (2), 166-175.

74. SciFinder, Chemical Abstracts Service. Accessed 2012-09-13

75. Rostovtsev, V. V.; Green, L. G.; Fokin, V. V.; Sharpless, K. B., A Stepwise Huisgen Cycloaddition Process: Copper(I)-Catalyzed Regioselective "Ligation" of Azides and Terminal Alkynes. *Angew. Chem., Int. Ed.* **2002,** *41* (14), 2596-2599.

76. Tornøe, C. W.; Christensen, C.; Meldal, M., Peptidotriazoles on Solid Phase: [1,2,3]-Triazoles by Regiospecific Copper(I)-Catalyzed 1,3-Dipolar Cycloadditions of Terminal Alkynes to Azides. *J. Org. Chem.* **2002,** *67* (9), 3057-3064.

77. Glimsdal, E.; Dragland, I.; Carlsson, M.; Eliasson, B.; Melø, T. B.; Lindgren, M., Triplet Excited States of Some Thiophene and Triazole Substituted Platinum(II) Acetylide Chromophores. *J. Phys. Chem. A* **2009,** *113* (14), 3311-3320.

78. Westlund, R.; Malmstrom, E.; Lopes, C.; Ohgren, J.; Rodgers, T.; Saito, Y.; Kawata, S.; Glimsdal, E.; Lindgren, M., Efficient nonlinear absorbing platinum(II) acetylide chromophores in solid PMMA matrices. *Adv. Funct. Mater.* **2008,** *18* (13), 1939-1948.

79. Chaumel, F.; Jiang, H. W.; Kakkar, A., Sol-gel materials for second-order nonlinear optics. *Chem. Mater.* **2001,** *13* (10), 3389-3395.

80. Siouffi, A. M., Silica gel-based monoliths prepared by the sol–gel method: facts and figures. *J. Chromatogr. A* **2003,** *1000* (1–2), 801-818.

81. Nguyen, K. A.; Kennel, J.; Pachter, R., A density functional theory study of phosphorescence and triplet-triplet absorption for nonlinear absorption chromophores. *J. Chem. Phys.* **2002,** *117* (15), 7128-7136.

82. Cronstrand, P.; Rinkevicius, Z.; Luo, Y.; Agren, H., Time-dependent density-functional theory calculations of triplet-triplet absorption. *J. Chem. Phys.* **2005,** *122* (22), 224104.

83. Norman, P., A perspective on nonresonant and resonant electronic response theory for time-dependent molecular properties. *Phys. Chem. Chem. Phys.* **2011,** *13* (46), 20519-20535.

84. Peach, M. J. G.; Benfield, P.; Helgaker, T.; Tozer, D. J., Excitation energies in density functional theory: An evaluation and a diagnostic test. *J. Chem. Phys.* **2008,** *128* (4), 044118.